US009808222B2

(12) **United States Patent**
Moore et al.

(10) **Patent No.: US 9,808,222 B2**
(45) **Date of Patent: Nov. 7, 2017**

(54) **INTRAVASCULAR ULTRASOUND SYSTEM FOR CO-REGISTERED IMAGING**

(75) Inventors: **Thomas C. Moore**, Livermore, CA (US); **Kendall R. Waters**, Livermore, CA (US); **J. Steve Reynolds**, Palo Alto, CA (US); **Duc H. Lam**, San Jose, CA (US); **Donald Masters**, San Diego, CA (US)

(73) Assignee: **ACIST Medical Systems, Inc.**, Eden Prairie, MN (US)

(*) Notice: Subject to any disclaimer, the term of this patent is extended or adjusted under 35 U.S.C. 154(b) by 945 days.

(21) Appl. No.: **12/902,460**

(22) Filed: **Oct. 12, 2010**

(65) **Prior Publication Data**

US 2011/0087104 A1 Apr. 14, 2011

Related U.S. Application Data

(60) Provisional application No. 61/250,781, filed on Oct. 12, 2009, provisional application No. 61/256,543, filed on Oct. 30, 2009.

(51) **Int. Cl.**
A61B 8/00 (2006.01)
A61B 8/12 (2006.01)
(Continued)

(52) **U.S. Cl.**
CPC ***A61B 8/4461*** (2013.01); ***A61B 8/0891*** (2013.01); ***A61B 8/12*** (2013.01);
(Continued)

(58) **Field of Classification Search**
CPC A61B 5/06; A61B 8/0833; A61B 8/0891; A61B 8/12; A61B 8/445; A61B 8/4461;
(Continued)

(56) **References Cited**

U.S. PATENT DOCUMENTS

4,347,443 A 8/1982 Whitney
4,850,363 A 7/1989 Yanagawa
(Continued)

FOREIGN PATENT DOCUMENTS

CN 101208045 A 6/2008
EP 0346889 A1 12/1989
(Continued)

OTHER PUBLICATIONS

Extended European Search Report dated Apr. 17, 2013 for EP Application No. 10823924.5, 6 pages.
(Continued)

Primary Examiner — Amanda Lauritzen Moher
(74) *Attorney, Agent, or Firm* — Fredrikson & Byron, P.A.

(57) **ABSTRACT**

An intravascular ultrasound imaging system with a catheter having an elongated body having a distal end and an imaging core arranged to be inserted into the elongated body. The imaging core is arranged to transmit ultrasonic energy pulses and to receive reflected ultrasonic energy pulses. The system further includes an imaging engine coupled to the imaging core and arranged to provide the imaging core with energy pulses to cause the imaging core to transmit the ultrasonic energy pulses. The energy pulses are arranged in repeated sequences and the energy pulses of each sequence have varying characteristics. The reflected pulses may be processed to provide a composite image of images resulting from each different characteristic.

11 Claims, 23 Drawing Sheets

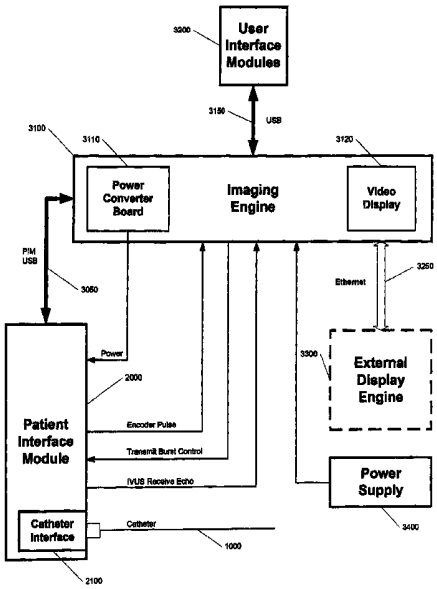

(51) **Int. Cl.**

G01S 7/52	(2006.01)
A61B 8/08	(2006.01)
G01S 15/10	(2006.01)
G01S 15/89	(2006.01)
A61B 5/06	(2006.01)

(52) **U.S. Cl.**

CPC ***A61B 8/445*** (2013.01); ***A61B 8/463*** (2013.01); ***G01S 7/52071*** (2013.01); ***G01S 7/52074*** (2013.01); *A61B 5/06* (2013.01); *A61B 8/0833* (2013.01); *G01S 15/102* (2013.01); *G01S 15/8952* (2013.01)

(58) **Field of Classification Search**

CPC ... A61B 8/463; G01S 15/102; G01S 15/8952; G01S 7/52071; G01S 7/52074

See application file for complete search history.

(56) **References Cited**

U.S. PATENT DOCUMENTS

4,860,758	A	8/1989	Yanagawa et al.	
4,949,310	A	8/1990	Smith et al.	
5,070,734	A	12/1991	Kawabuchi et al.	
5,131,396	A	7/1992	Ishiguro et al.	
5,183,048	A	2/1993	Eberle	
5,203,338	A	4/1993	Jang	
5,363,849	A	11/1994	Suorsa et al.	
5,396,285	A	3/1995	Hedberg et al.	
5,462,057	A	10/1995	Hunt et al.	
5,531,679	A	7/1996	Schulman et al.	
5,690,115	A	11/1997	Feldman et al.	
5,741,552	A	4/1998	Takayama et al.	
5,833,615	A	11/1998	Wu et al.	
5,848,969	A	12/1998	Panescu et al.	
5,876,343	A *	3/1999	Teo	A61B 8/12 600/443
6,015,385	A	1/2000	Finger et al.	
6,132,374	A	10/2000	Hossack et al.	
6,139,501	A	10/2000	Roundhill et al.	
6,154,572	A	11/2000	Chaddha	
6,216,025	B1	4/2001	Kruger	
6,277,075	B1	8/2001	Torp et al.	
6,454,715	B2 *	9/2002	Teo	A61B 8/06 600/443
6,589,181	B2	7/2003	Grunwald et al.	
6,645,147	B1	11/2003	Jackson et al.	
7,194,294	B2	3/2007	Panescu et al.	
7,691,061	B2	4/2010	Hirota	
7,925,064	B2	4/2011	Cloutier et al.	
2001/0017941	A1	8/2001	Chaddha	
2001/0029336	A1	10/2001	Ieo	
2003/0063787	A1 *	4/2003	Natanzon	G01T 1/1615 382/131
2003/0078497	A1 *	4/2003	Ji et al.	600/437
2003/0097069	A1	5/2003	Avinash et al.	
2003/0191392	A1	10/2003	Haldeman	
2003/0208123	A1	11/2003	Panescu	
2004/0030250	A1	2/2004	Stewart	
2004/0037164	A1 *	2/2004	Garlick et al.	367/8
2004/0199047	A1	10/2004	Taimisio et al.	
2005/0215897	A1	9/2005	Sakaguchi et al.	
2005/0249391	A1	11/2005	Kimmel et al.	
2006/0253028	A1	11/2006	Lam et al.	
2007/0016068	A1 *	1/2007	Grunwald et al.	600/468
2007/0036404	A1	2/2007	Li	
2007/0167710	A1	7/2007	Unal et al.	
2008/0015569	A1 *	1/2008	Saadat et al.	606/41
2008/0031498	A1	2/2008	Corcoran et al.	
2008/0200815	A1	8/2008	Van Der Sieen et al.	
2009/0088830	A1 *	4/2009	Mohamed et al.	623/1.11
2009/0284332	A1	11/2009	Moore et al.	
2010/0010344	A1	1/2010	Ahn et al.	
2010/0094127	A1	4/2010	Xu	
2010/0174190	A1	7/2010	Hancock et al.	
2010/0312109	A1	12/2010	Satoh	
2011/0071404	A1	3/2011	Schmitt et al.	
2011/0160586	A1	6/2011	Li et al.	
2012/0065511	A1	3/2012	Jamello, III	
2012/0123271	A1	5/2012	Cai	
2012/0170848	A1	7/2012	Kemp et al.	
2013/0109968	A1	5/2013	Azuma	
2013/0303907	A1	11/2013	Corl	
2013/0303910	A1	11/2013	Hubbard et al.	
2014/0180078	A1	6/2014	Nair	
2014/0276065	A1 *	9/2014	He	A61B 8/5207 600/445
2015/0099975	A1	4/2015	Lam et al.	
2015/0141832	A1	5/2015	Yu et al.	

FOREIGN PATENT DOCUMENTS

EP	851241	A2	7/1998
EP	1387317	A1	2/2004
EP	1609423	A2	12/2005
EP	10823924.5		4/2011
JP	2009000522		1/1997
JP	2001333902	A	12/2001
JP	2002530143	A	9/2002
JP	2004180784		7/2004
JP	2006-014938		1/2006
JP	2007029520	A	2/2007
JP	2007175542	A	7/2007
JP	2007229015	A	9/2007
JP	2008508970	A	3/2008
JP	2008536638	A	9/2008
JP	2009545406	A	12/2009
JP	4648652	B2	3/2011
JP	2013507227	A	3/2013
WO	0101864	A1	1/2001
WO	WO2006015877	A1	2/2006
WO	WO2006113857	A1	10/2006
WO	2006122001	A2	11/2006
WO	2007098209	A2	8/2007
WO	2008016992	A1	2/2008
WO	2008110013	A1	9/2008
WO	2011046903	A1	4/2011
WO	2014186268	A1	11/2014

OTHER PUBLICATIONS

Van Der Steen A.F.W. et al.: "IVUS Harmonic Imaging," Ultrasound Med BIOL; Ultrasound in Medicine and Biology 2000 Elsevier Science LTD, Exter, Engl, vol. 26, No. supp. 2, 2000, p. A90.

Foster, F. Stuart: "Transcuder Materials and Probe Construction," Ultrasound in Medicine and Biology, New York, NY, US, vol. 26, May 2000, pp. S2-S5.

Frijlink, M.E. et al.: "High Frequency Harmonic Imaging in Presence of Intravascular Stents," IEEE Ultrasonics Symposium (IEEE CAT. No. 03CH37476) Piscataway, NJ, USA, vol. 1, 2003, pp. 208-211.

U.S. Appl. No. 61/218,177, filed Jun. 18, 2009 titled Vector Domain Image Enhancement for Mechnically Rotating Imaging Catheters.

Dumane et al., "Use of Frequency Diversity and Nakagami Statistics in Ultrasonic Tissue Characterization," IEEE Transactions on Ultrasonics, Ferroelectrics, and Frequency Control, vol. 48, No. 5, Sep. 2001, pp. 1139-1146.

Garcia-Garcia et al., "Imaging of coronary atherosclerosis: intravascular ultrasound," European Heart Journal, vol. 3, 2010, pp. 2456-2469.

International Patent Application No. PCT/US2010/052258, International Search Report & Written Opinion dated May 18, 2011, 6 pages.

Seo et al., "Sidelobe Suppression in Ultrasound Imaging Using Dual Apodization with Cross-Correlation," IEEE Transactions on Ultrasonics, Ferroelectrics, and Frequency Control, vol. 55, No. 10, Oct. 2008, pp. 2198-2210.

Shankar et al., "Computer-Aided Classification of Breast Masses in Ultrasonic B-Scans Using a Multiparameter Approach," IEEE

(56) **References Cited**

OTHER PUBLICATIONS

Transactions on Ultrasonics, Ferroelectrics, and Frequency Control, vol. 50, No. 8, Aug. 2003, pp. 1002-1009.
Smith et al., "The Maltese Cross Processor: Speckle Reduction for Circular Transducers," Ultrasonic Imaging, vol. 10, No. 3, Jul. 1988, pp. 153-170.
Wang et al., "Optimizing the Beam Pattern of a Forward-Viewing Ring-Annular Ultrasound Array for Intravascular Imaging," IEEE Transactions on Ultrasonics, Ferroelectrics, and Frequency Control, vol. 49, No. 12, Dec. 2002, pp. 1652-1664.
Waters et al., "Development of a High-Definition Intravascular Ultrasound Imaging System and Catheter," IEEE International Ultrasonics Symposium Proceedings, Oct. 18, 2011, 4 pages.

* cited by examiner

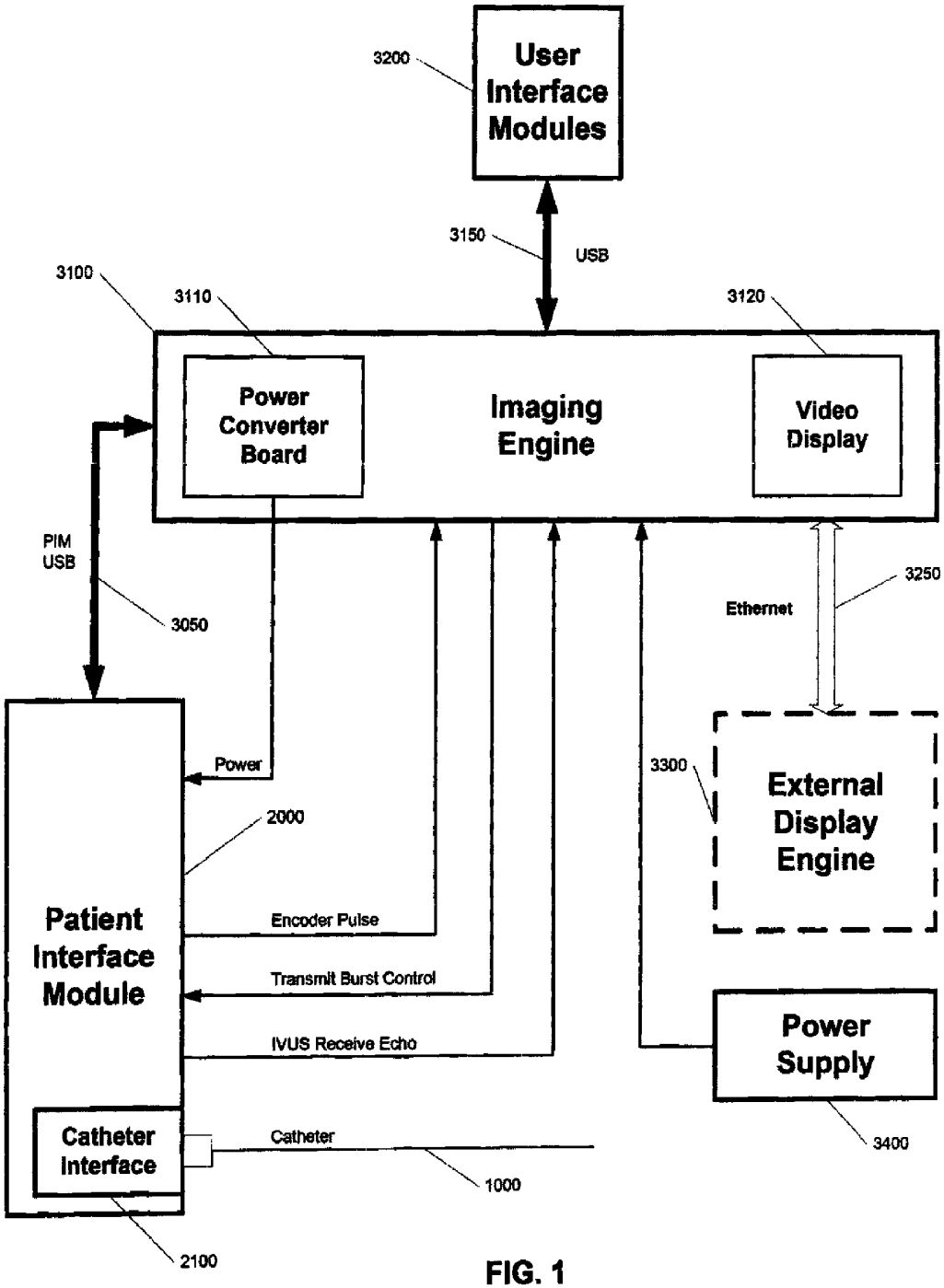
User Interface Modules
3200
3150
USB
3100
3110
3120
Power Converter Board
Imaging Engine
Video Display
PIM USB
3050
Ethernet
3250
Power
2000
3300
External Display Engine
Patient Interface Module
Encoder Pulse
Transmit Burst Control
IVUS Receive Echo
Power Supply
3400
Catheter Interface
Catheter
1000
2100

FIG. 1

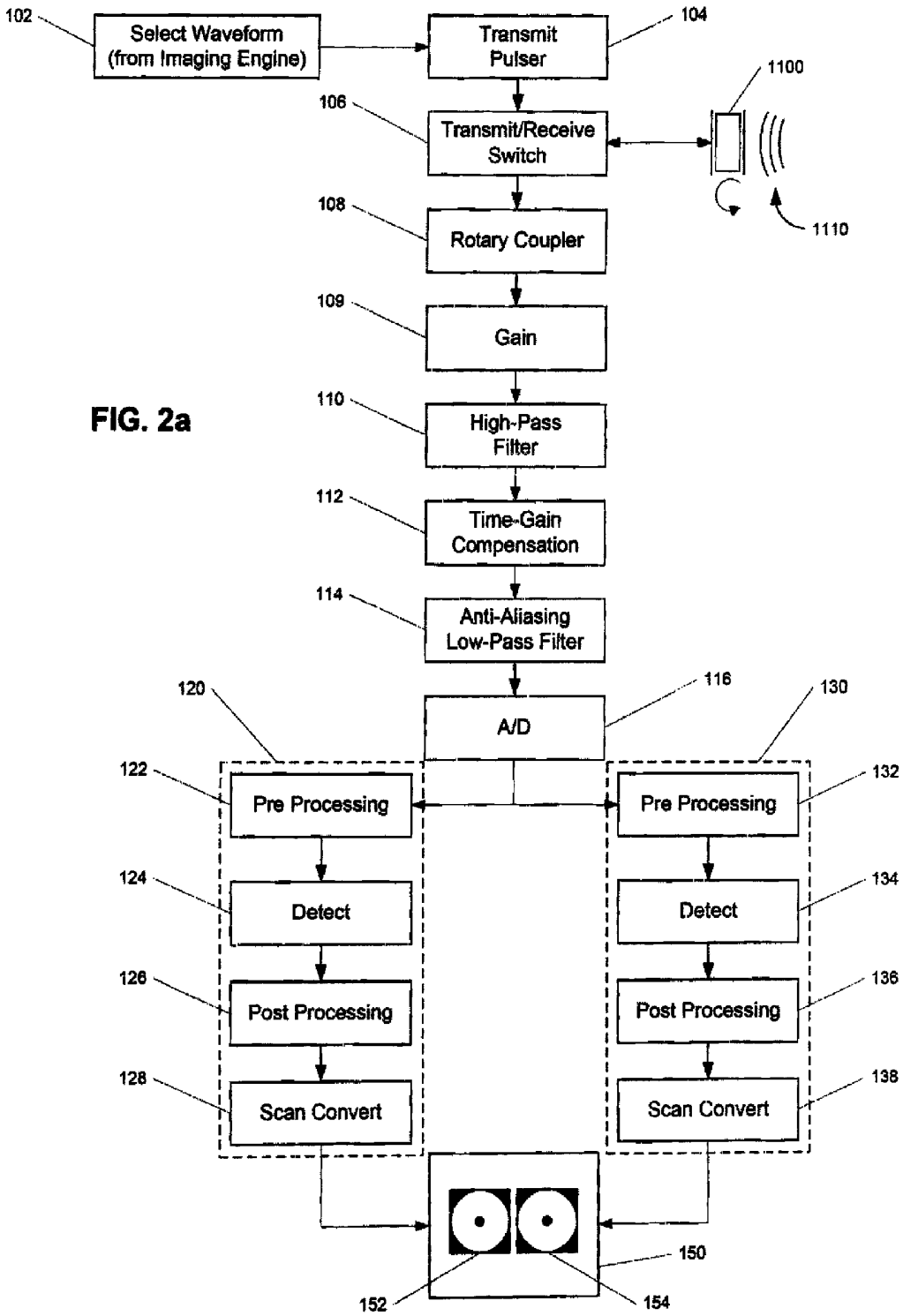
102
Select Waveform (from Imaging Engine)
Transmit Pulser
104
1100
106
Transmit/Receive Switch
1110
108
Rotary Coupler
109
Gain
110
High-Pass Filter
112
Time-Gain Compensation
114
Anti-Aliasing Low-Pass Filter
120
116
130
A/D
122
Pre Processing
132
Pre Processing
124
Detect
134
Detect
126
Post Processing
136
Post Processing
128
Scan Convert
138
Scan Convert
150
152
154

FIG. 2a

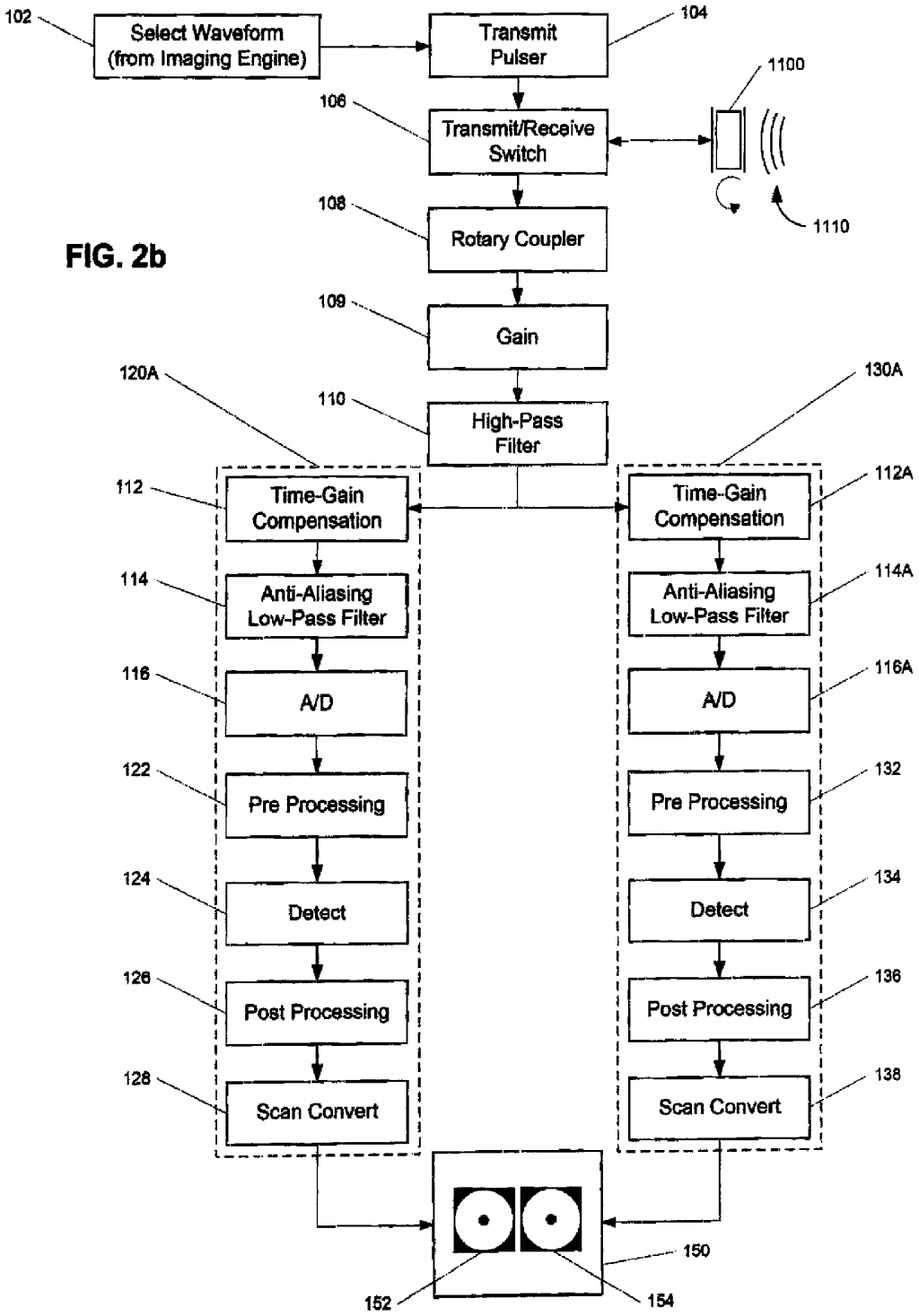
102
Select Waveform (from Imaging Engine)
Transmit Pulser
104
1100
106
Transmit/Receive Switch
1110
108
Rotary Coupler
109
Gain
120A
130A
110
High-Pass Filter
112
Time-Gain Compensation
112A
114
Anti-Aliasing Low-Pass Filter
114A
116
A/D
116A
122
Pre Processing
132
124
Detect
134
126
Post Processing
136
128
Scan Convert
138
150
152
154

FIG. 2b

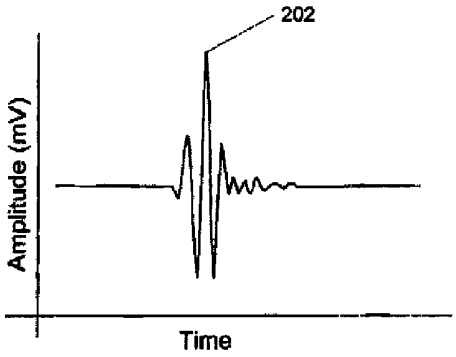

FIG. 3a

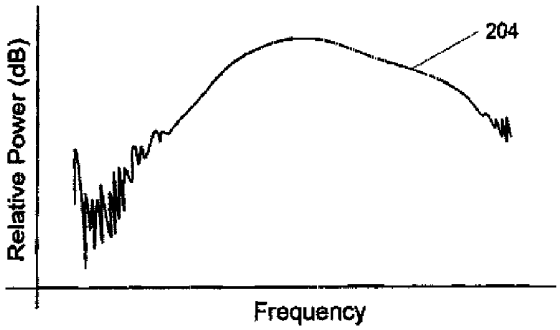

FIG. 3b

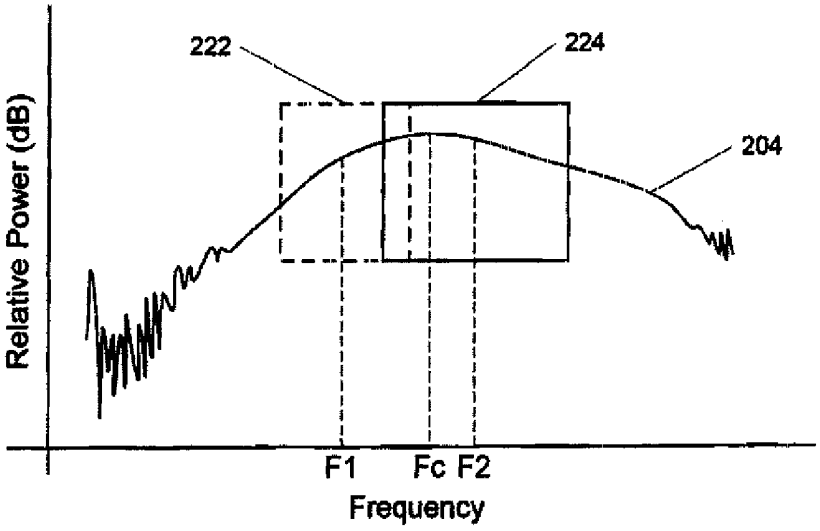
222
224
204
Relative Power (dB)
F1
Fc
F2
Frequency

FIG. 4a

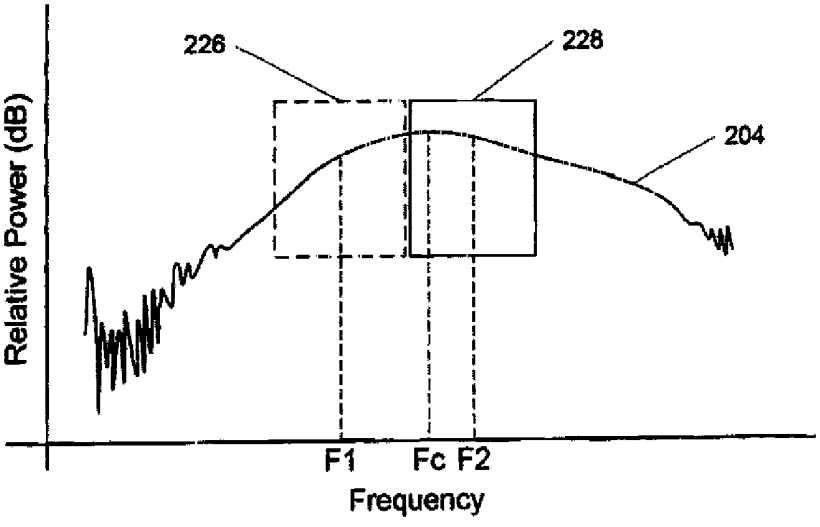
226
228
204
Relative Power (dB)
F1
Fc
F2
Frequency

FIG. 4b

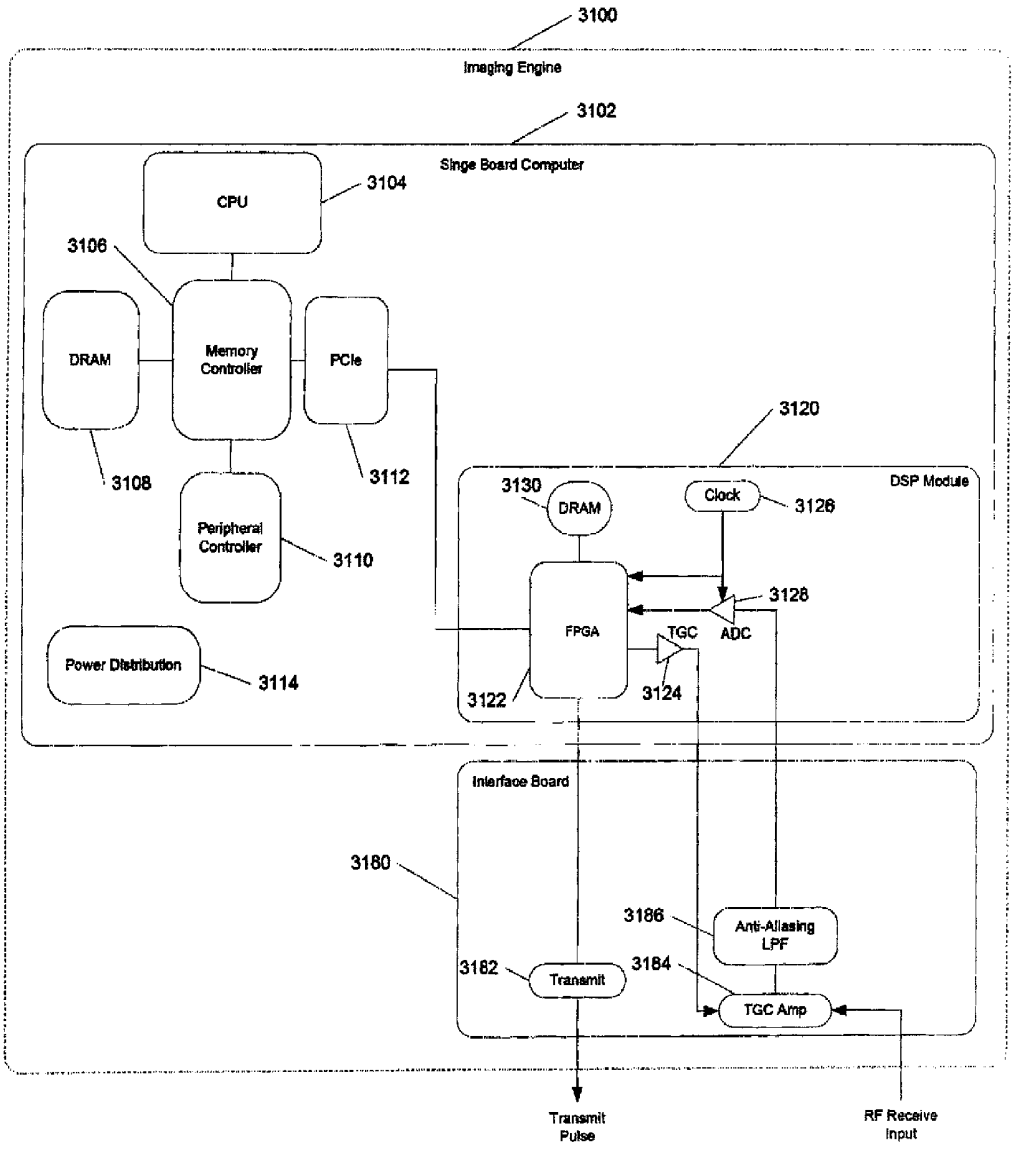
3100
Imaging Engine
3102
Singe Board Computer
CPU
3104
3106
DRAM
Memory Controller
PCIe
3108
3112
Peripheral Controller
3110
Power Distribution
3114
3120
DSP Module
3130
DRAM
Clock
3126
3128
FPGA
TGC
ADC
3122
3124
Interface Board
3180
3186
Anti-Aliasing LPF
3182
Transmit
3184
TGC Amp
Transmit Pulse
RF Receive Input

FIG. 5a

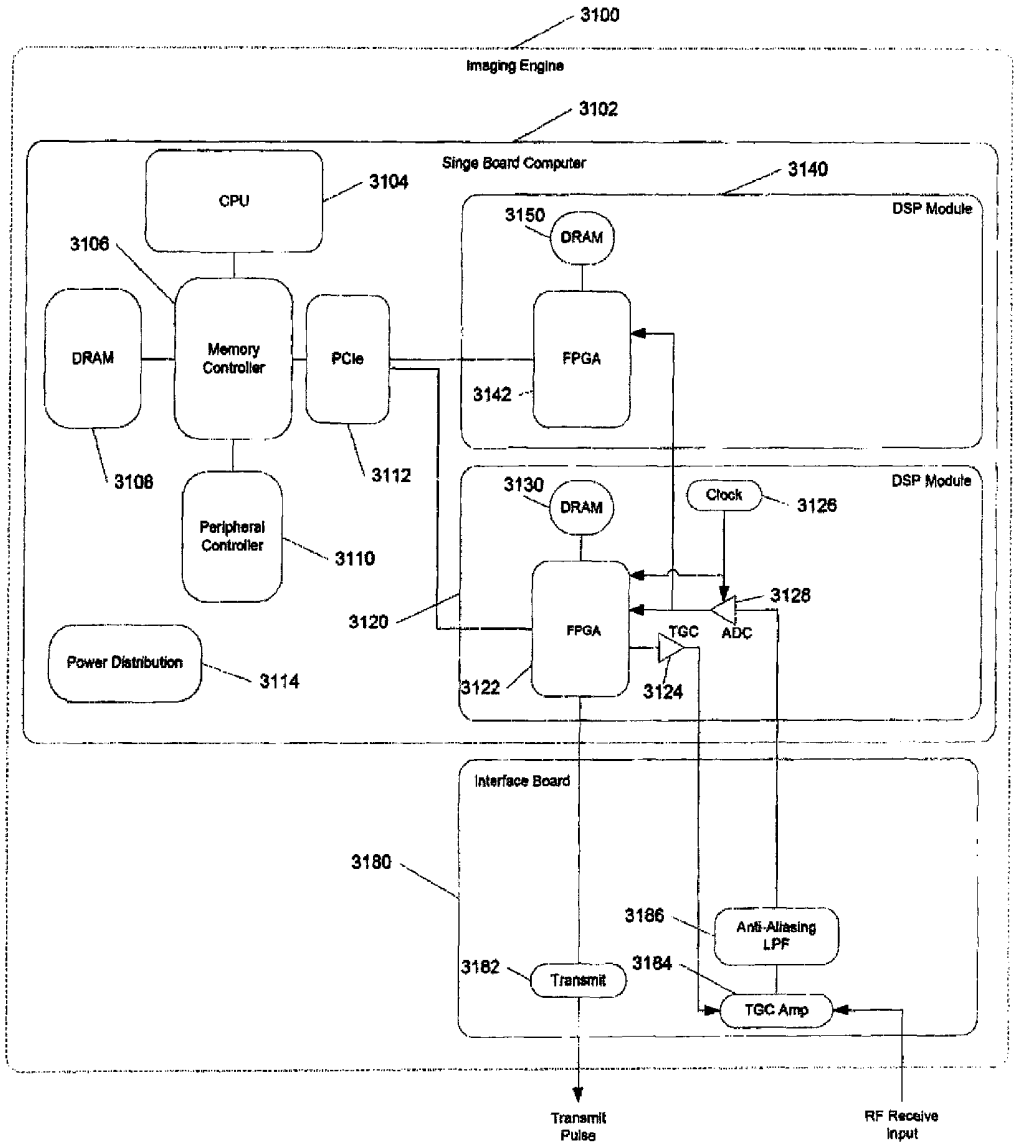
3100
Imaging Engine
3102
Singe Board Computer
CPU
3104
3106
DRAM
Memory Controller
PCIe
3108
3112
Peripheral Controller
3110
Power Distribution
3114
3120
3140
DSP Module
3150
DRAM
FPGA
3142
DSP Module
3130
DRAM
Clock
3126
3128
FPGA
TGC
ADC
3122
3124
Interface Board
3180
3186
Anti-Aliasing LPF
3182
Transmit
3184
TGC Amp
Transmit Pulse
RF Receive Input

FIG. 5b

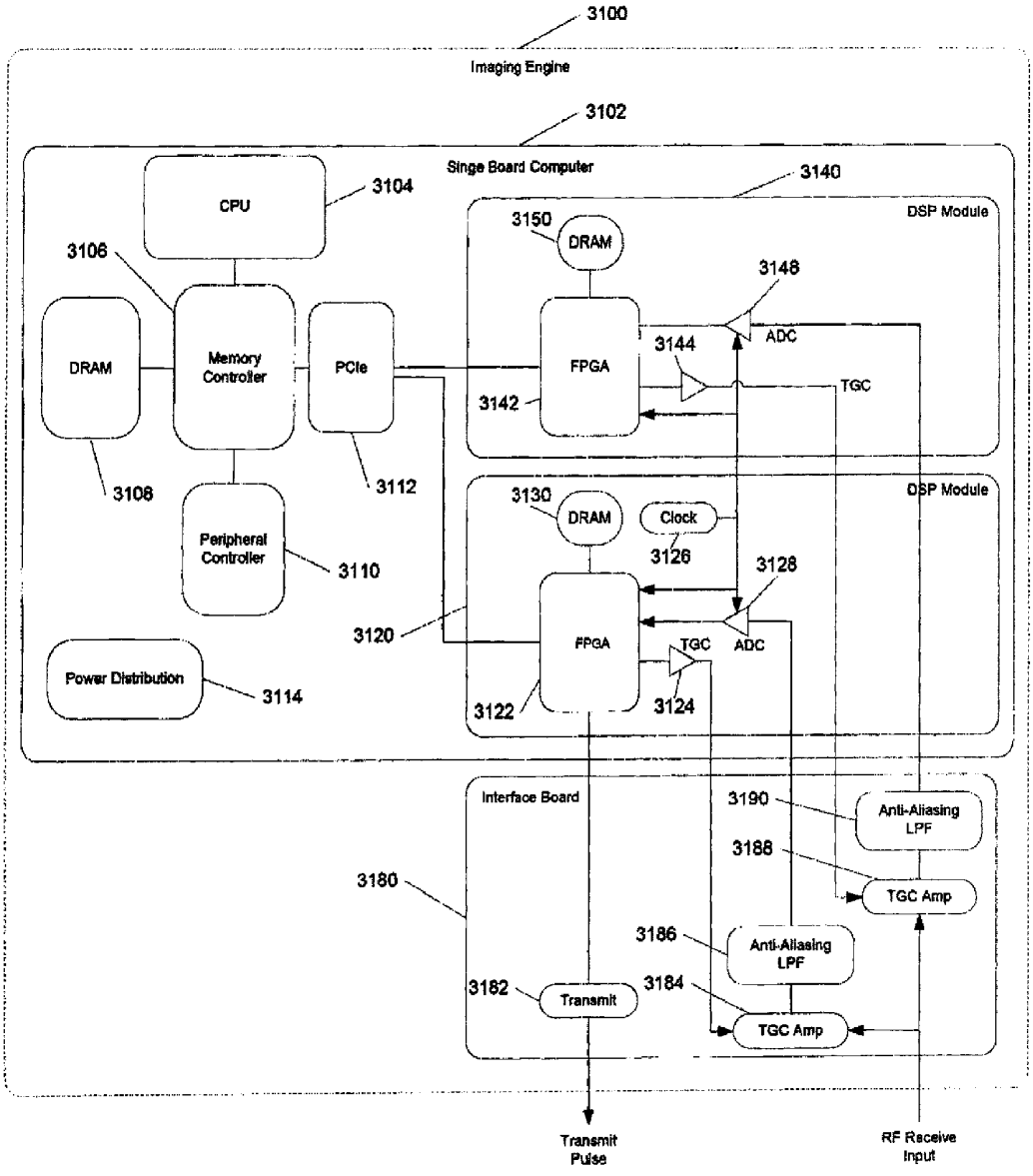
3100
Imaging Engine
3102
Singe Board Computer
CPU
3104
3106
DRAM
Memory Controller
PCIe
3108
3112
Peripheral Controller
3110
Power Distribution
3114
3140
DSP Module
3150
DRAM
3148
ADC
3144
FPGA
TGC
3142
DSP Module
3130
DRAM
Clock
3126
3128
3120
FPGA
TGC
ADC
3122
3124
Interface Board
3190
Anti-Aliasing LPF
3188
TGC Amp
3180
3186
Anti-Aliasing LPF
3182
Transmit
3184
TGC Amp
Transmit Pulse
RF Receive Input

FIG. 5c

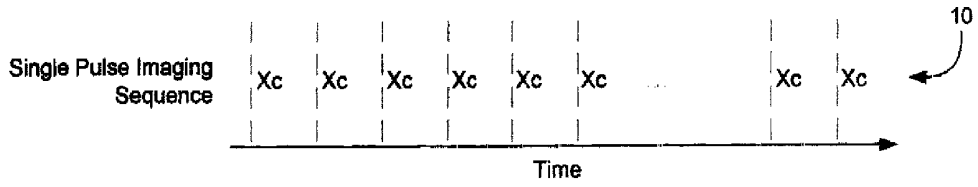

FIG. 6a

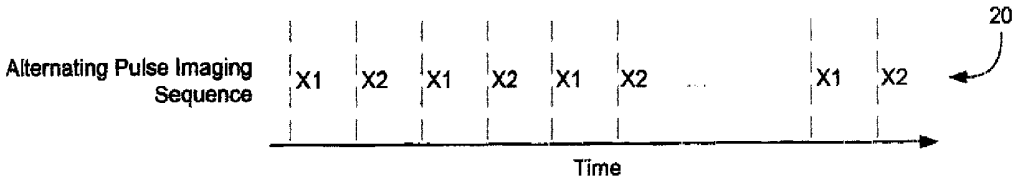

FIG. 6b

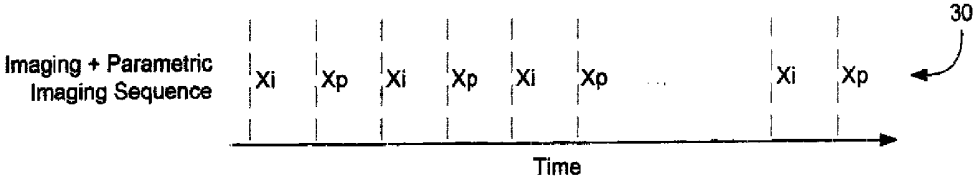

FIG. 6c

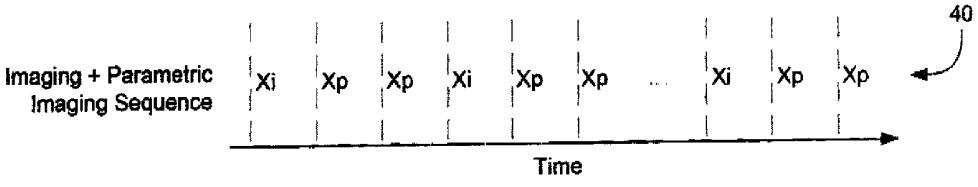

FIG. 6d

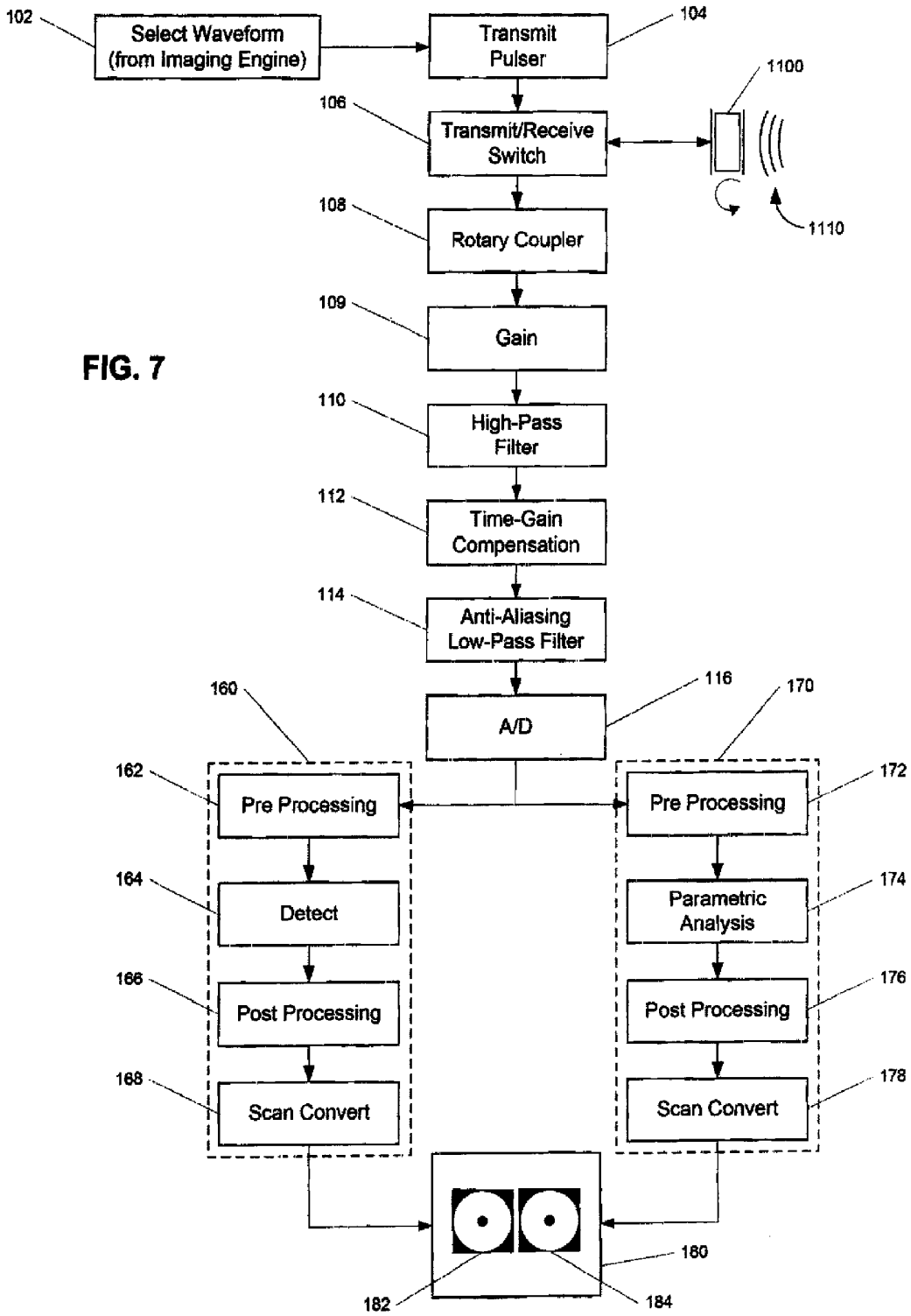
102
Select Waveform (from Imaging Engine)
104
Transmit Pulser
1100
106
Transmit/Receive Switch
1110
108
Rotary Coupler
109
Gain
110
High-Pass Filter
112
Time-Gain Compensation
114
Anti-Aliasing Low-Pass Filter
116
A/D
160
170
162
Pre Processing
164
Detect
166
Post Processing
168
Scan Convert
172
Pre Processing
174
Parametric Analysis
176
Post Processing
178
Scan Convert
180
182
184

FIG. 7

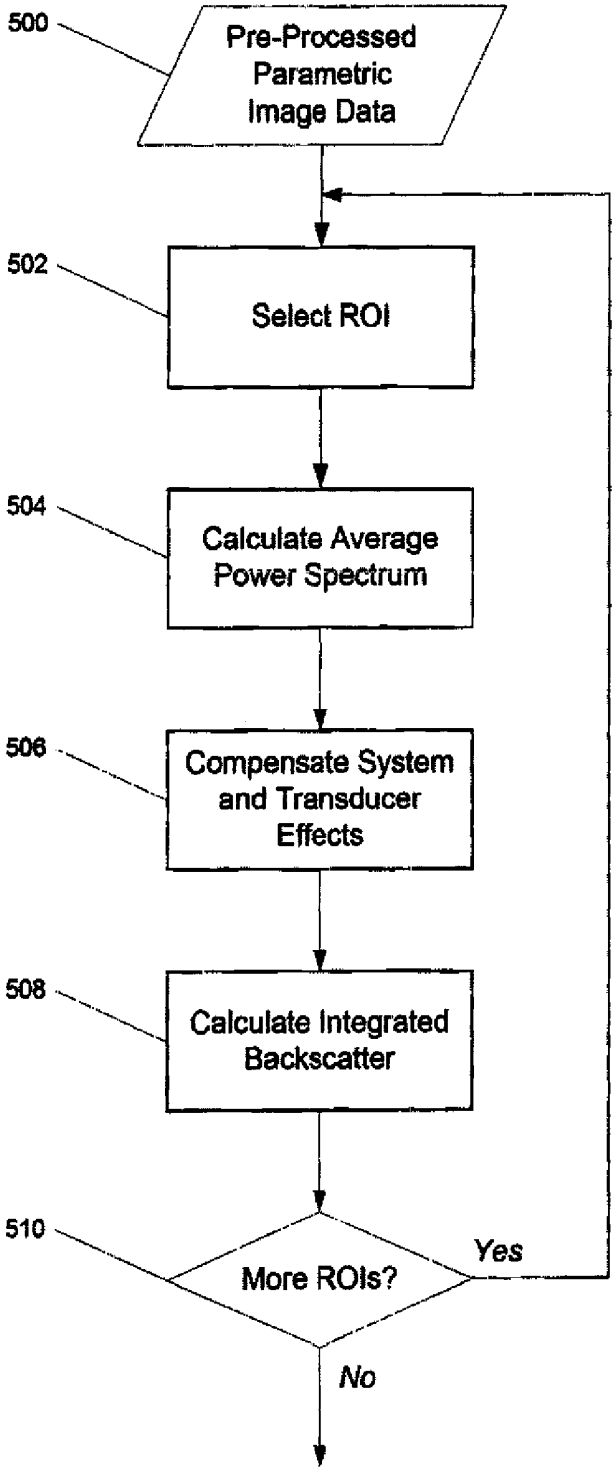
500
Pre-Processed Parametric Image Data
502
Select ROI
504
Calculate Average Power Spectrum
506
Compensate System and Transducer Effects
508
Calculate Integrated Backscatter
510
More ROIs?
Yes
No
To Parametric Image Analysis Post-Processing

FIG. 8

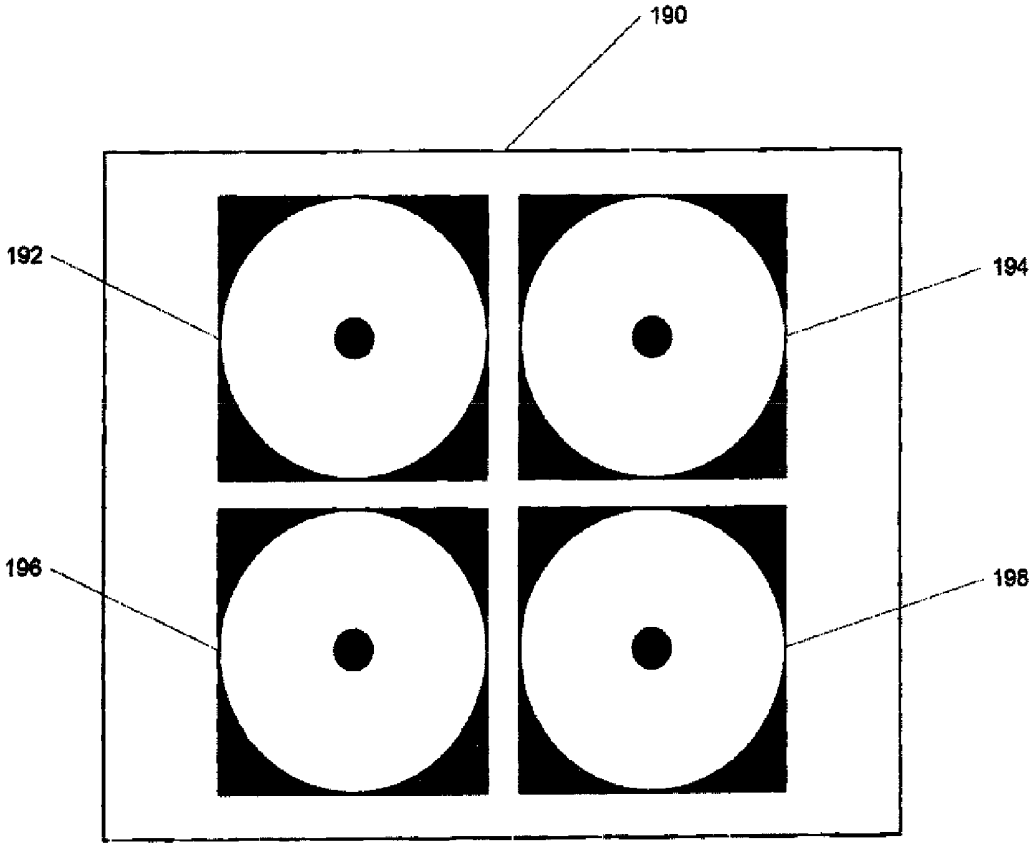

FIG. 9

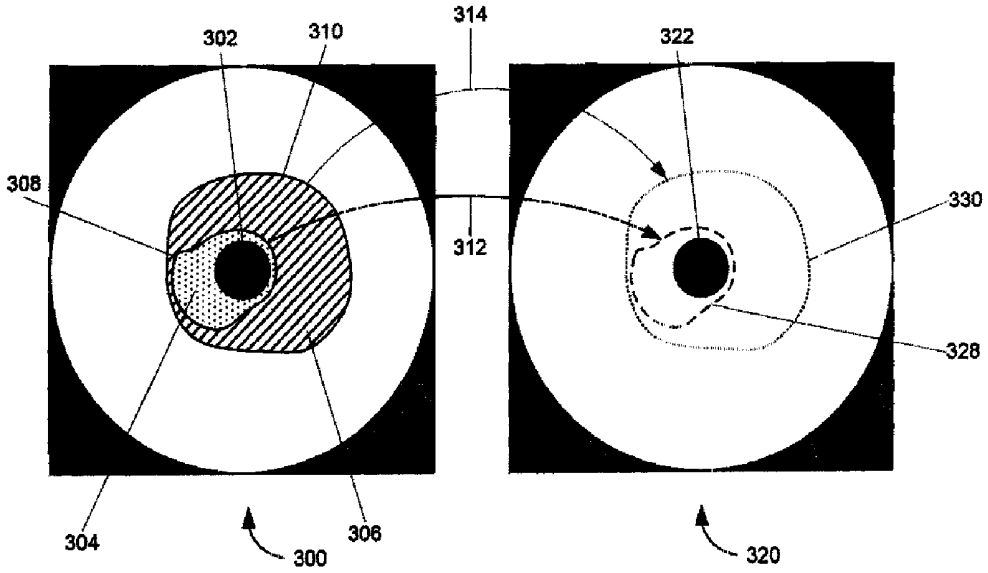

FIG. 10a

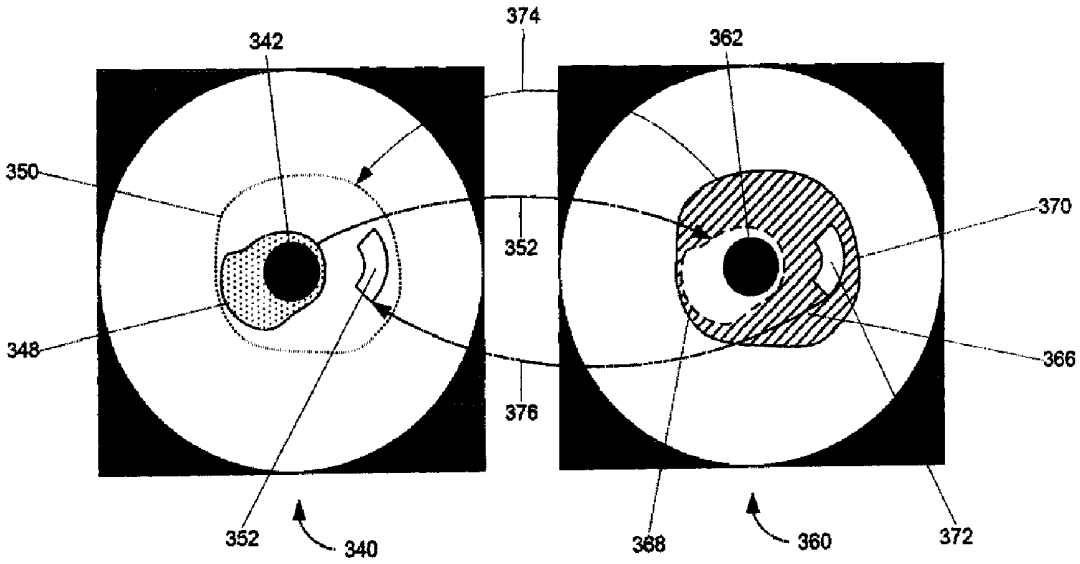

FIG. 10b

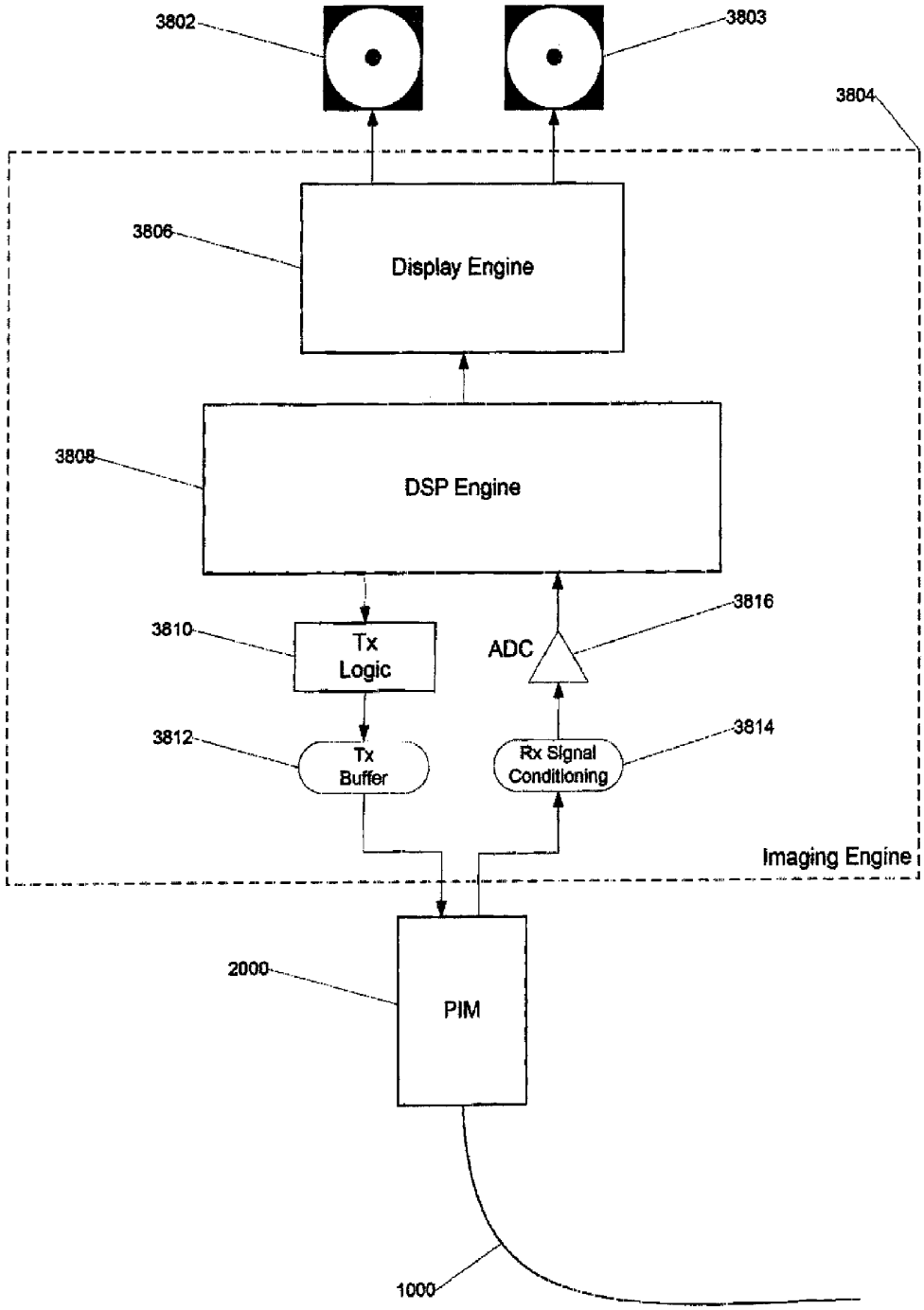
3802
3803
3804
3806
Display Engine
3808
DSP Engine
3810
Tx Logic
ADC
3816
3812
Tx Buffer
Rx Signal Conditioning
3814
Imaging Engine
2000
PIM
1000

FIG. 11

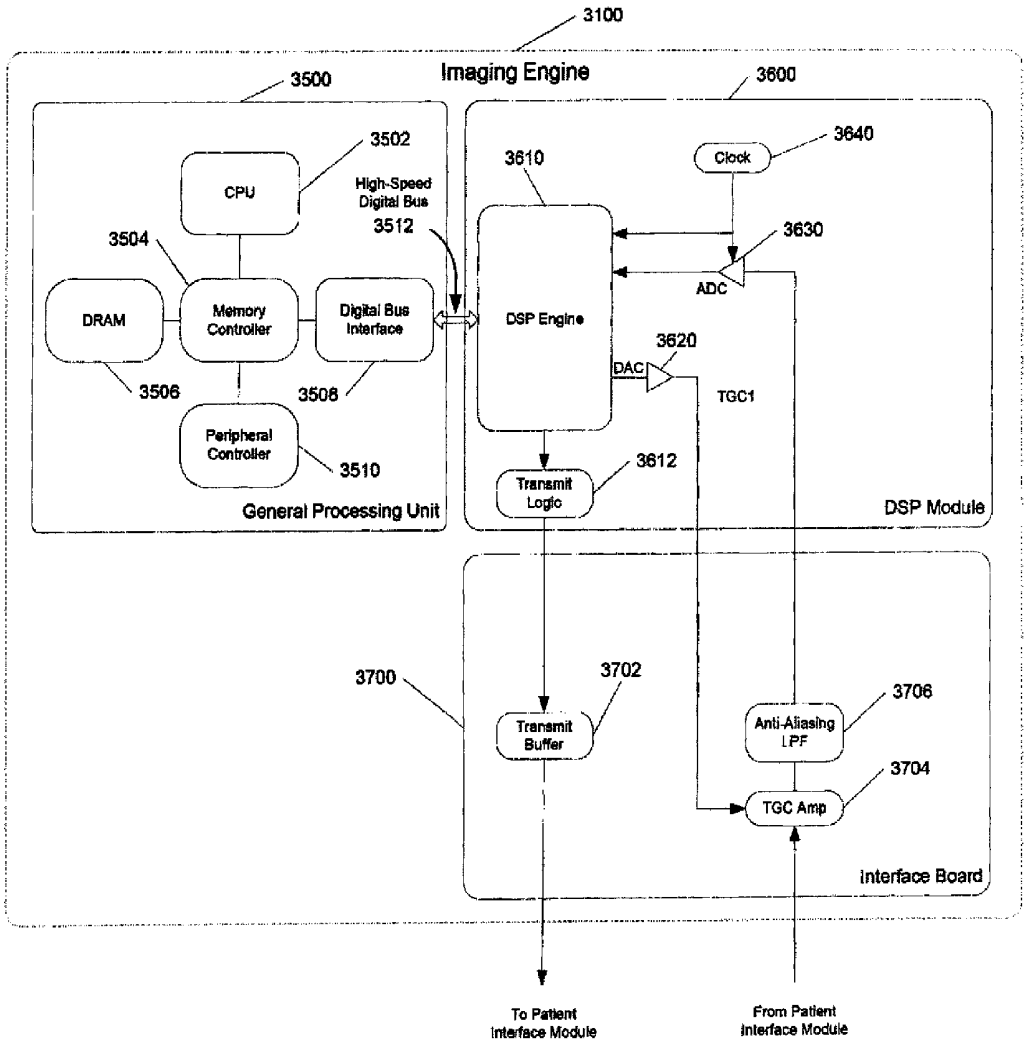
3100
Imaging Engine
3500
3600
3502
CPU
High-Speed Digital Bus
3512
3504
DRAM
Memory Controller
Digital Bus Interface
3506
3508
Peripheral Controller
3510
General Processing Unit
3610
Clock
3640
3630
ADC
DSP Engine
3620
DAC
TGC1
3612
Transmit Logic
DSP Module
3700
3702
Transmit Buffer
3706
Anti-Aliasing LPF
3704
TGC Amp
Interface Board
To Patient Interface Module
From Patient Interface Module

FIG. 12

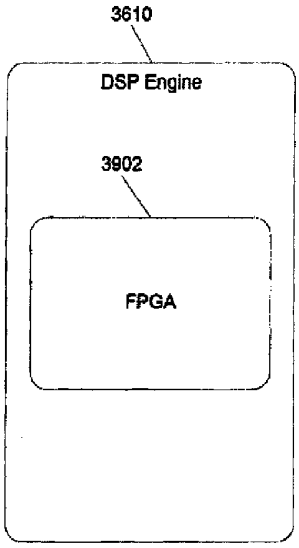

FIG. 13

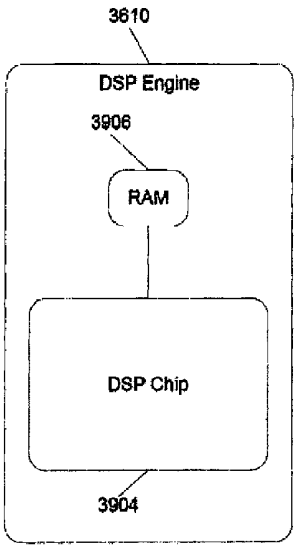

FIG. 14

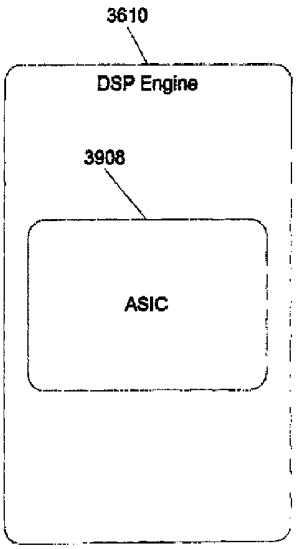

FIG. 15

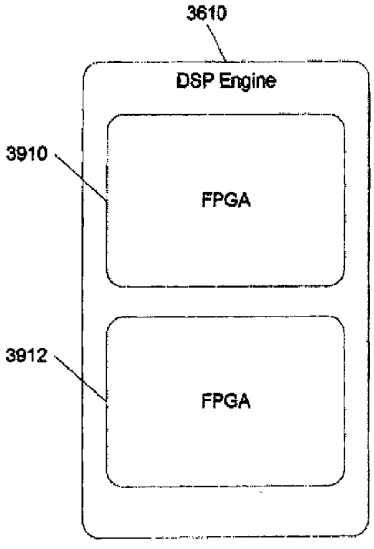

FIG. 16

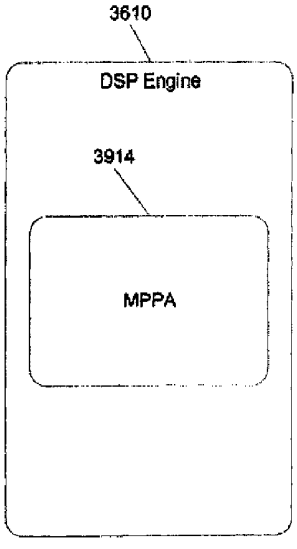

FIG. 17

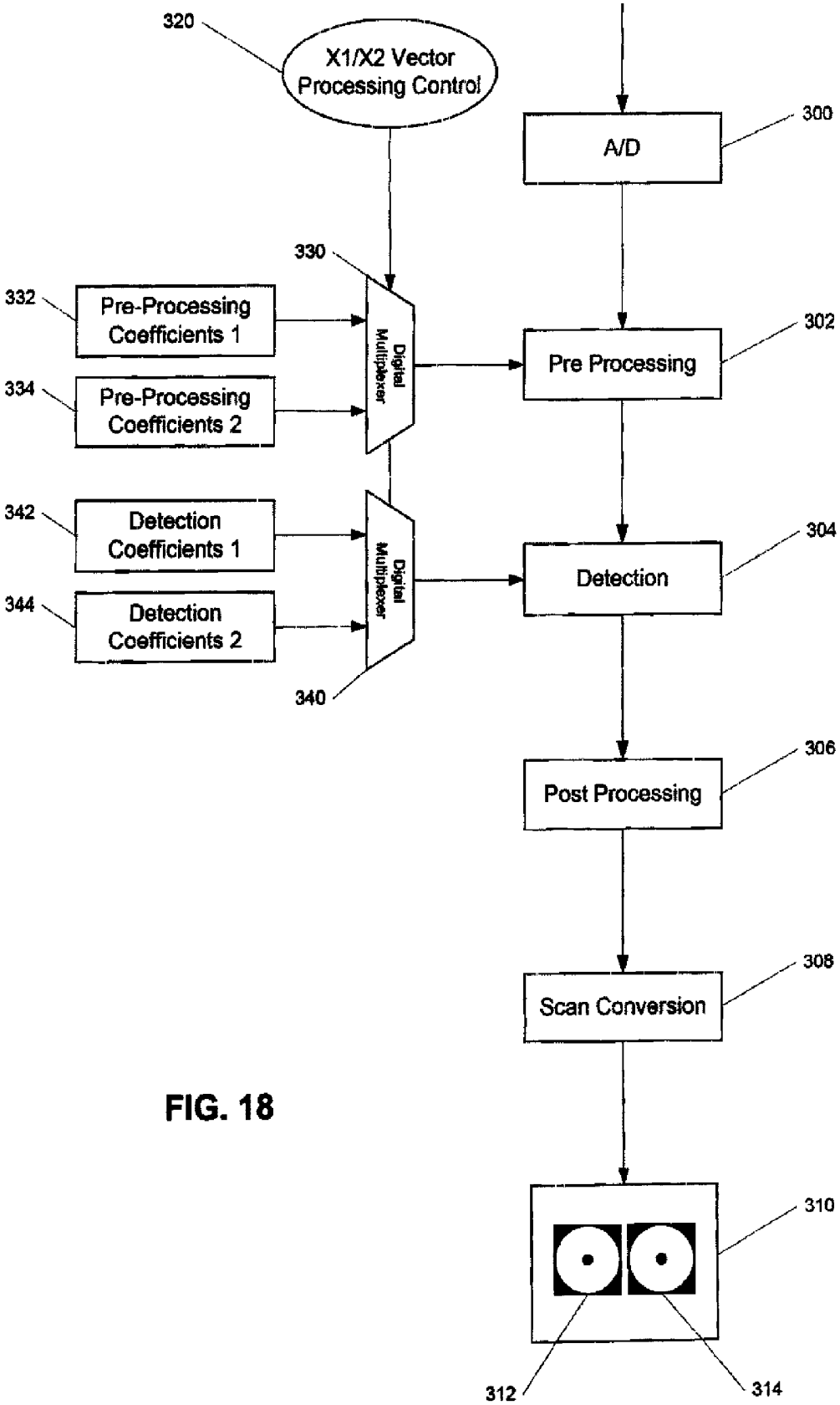
320
X1/X2 Vector Processing Control
A/D
300
330
332
Pre-Processing Coefficients 1
334
Pre-Processing Coefficients 2
Digital Multiplexer
Pre Processing
302
342
Detection Coefficients 1
344
Detection Coefficients 2
Digital Multiplexer
Detection
304
340
Post Processing
306
Scan Conversion
308
310
312
314

FIG. 18

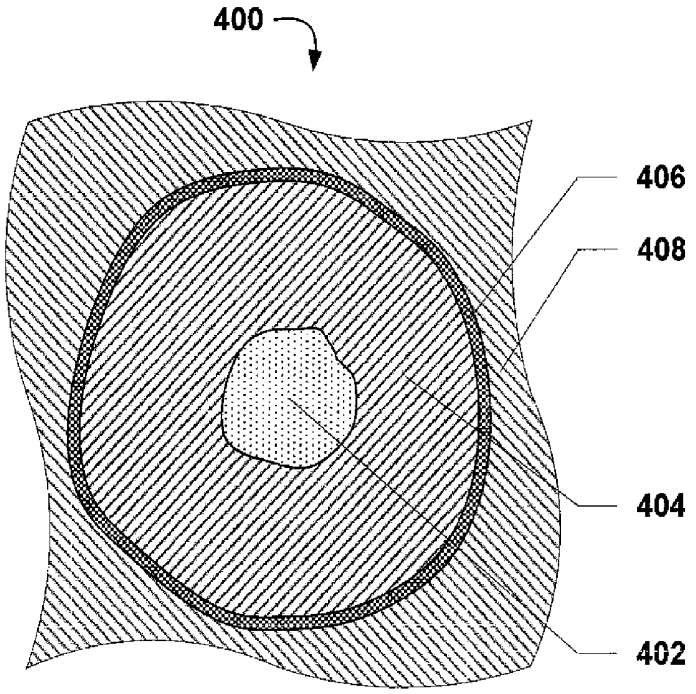

FIG. 19

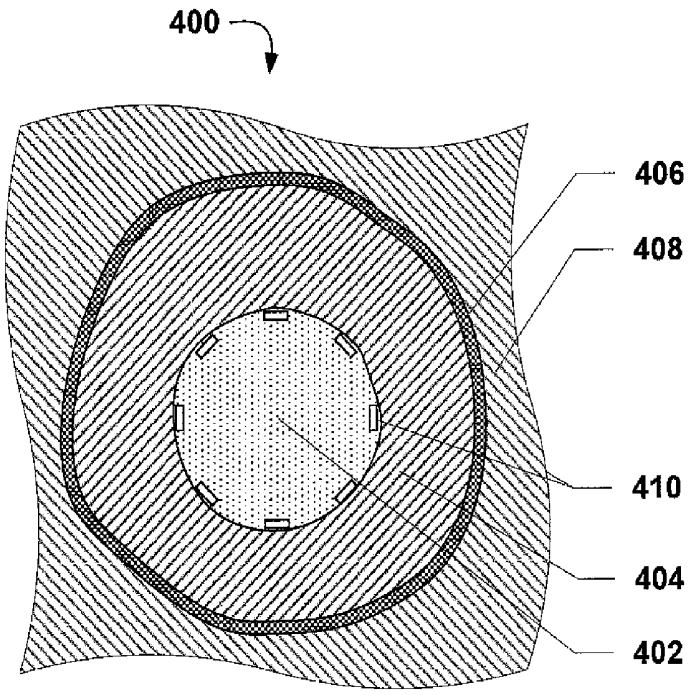

FIG. 20

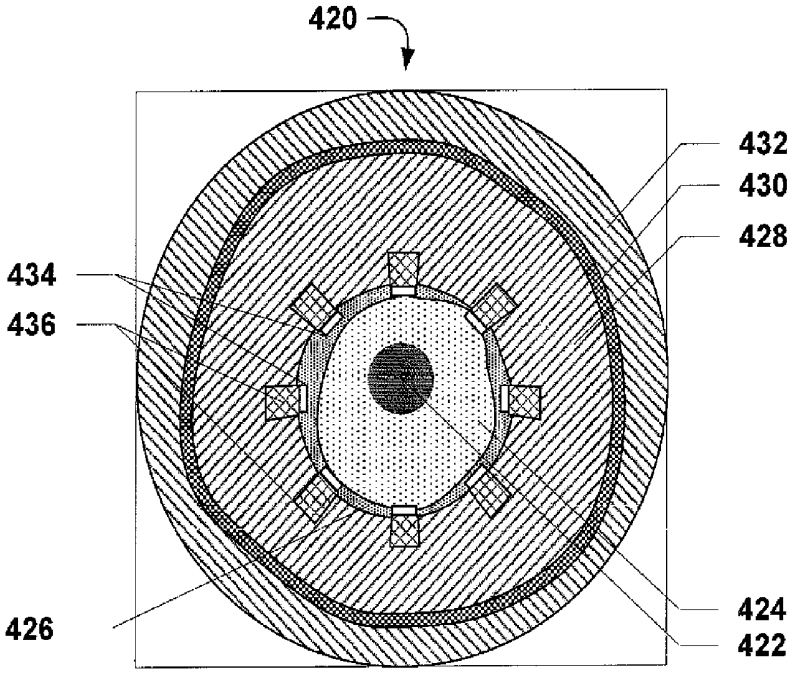
420
432
430
428
434
436
426
424
422

FIG. 21

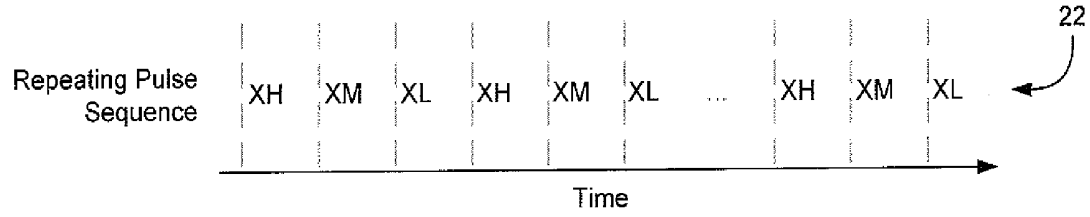
22
Repeating Pulse Sequence
XH
XM
XL
XH
XM
XL
...
XH
XM
XL
Time

FIG. 22

FIG. 23

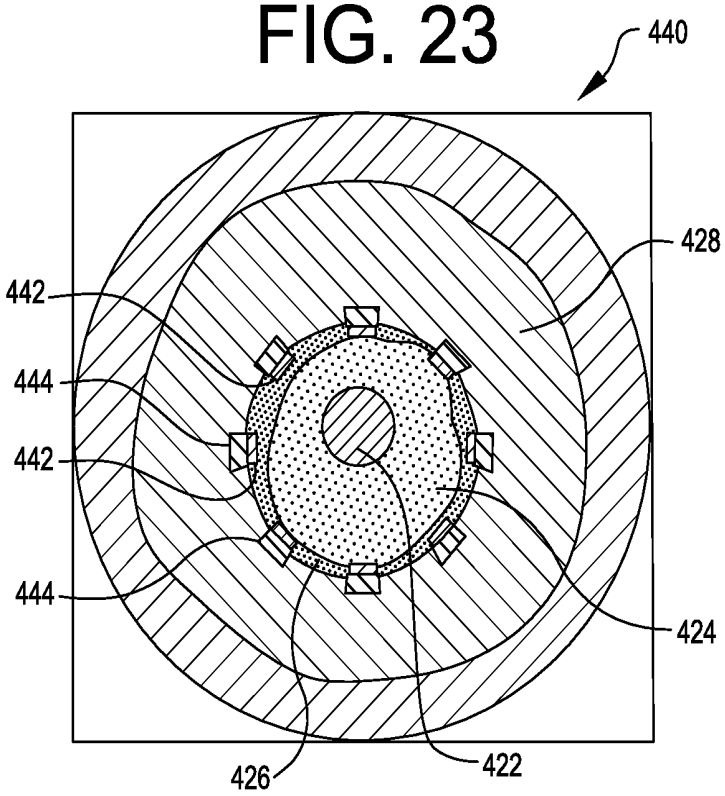

FIG. 24

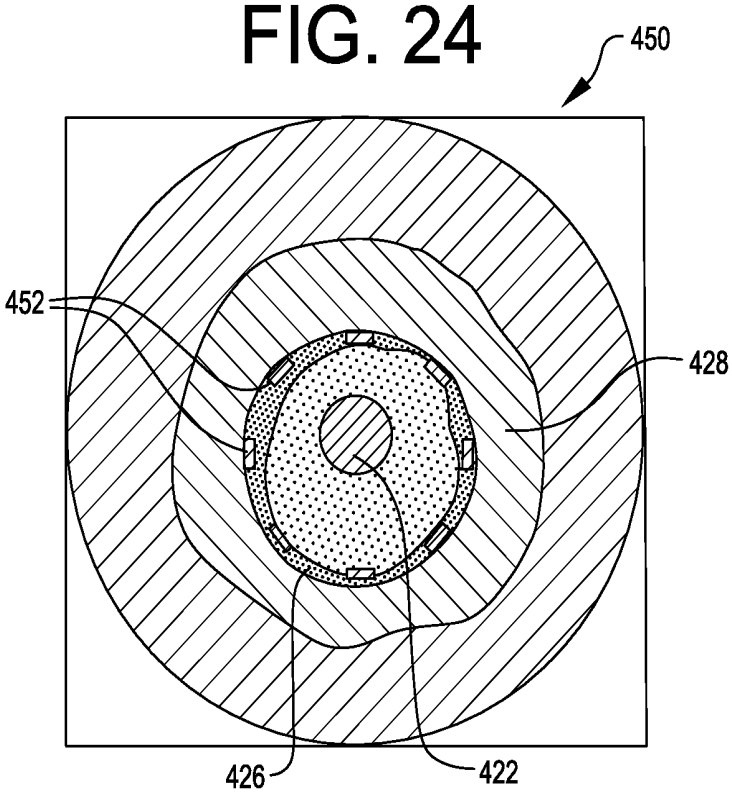

FIG. 25

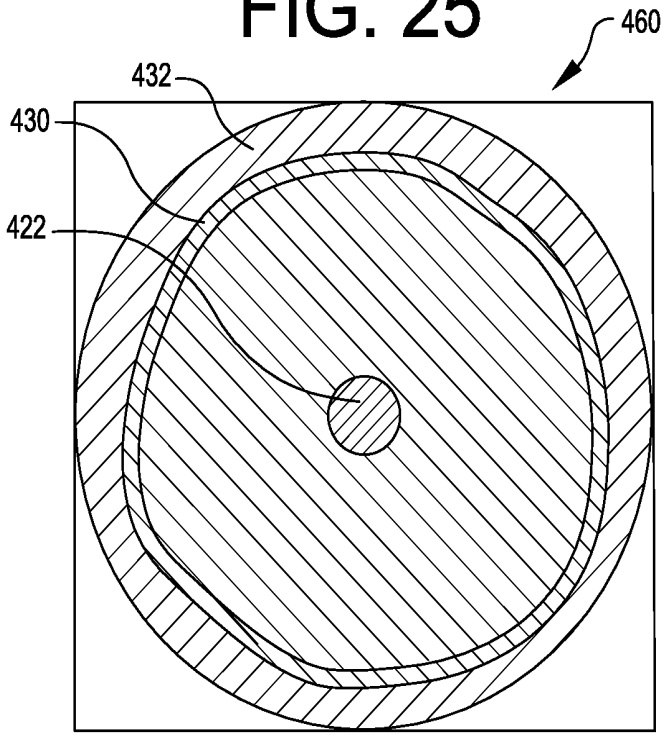

FIG. 26

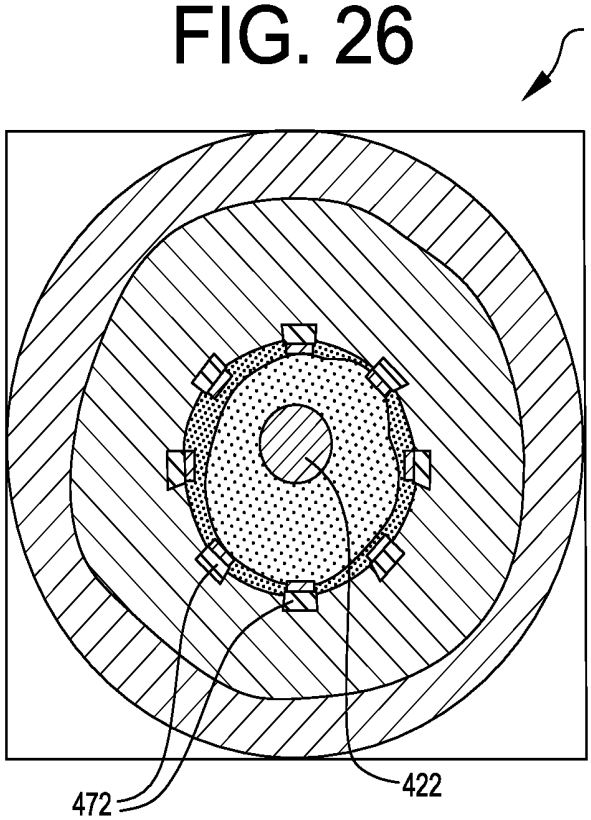

FIG. 27

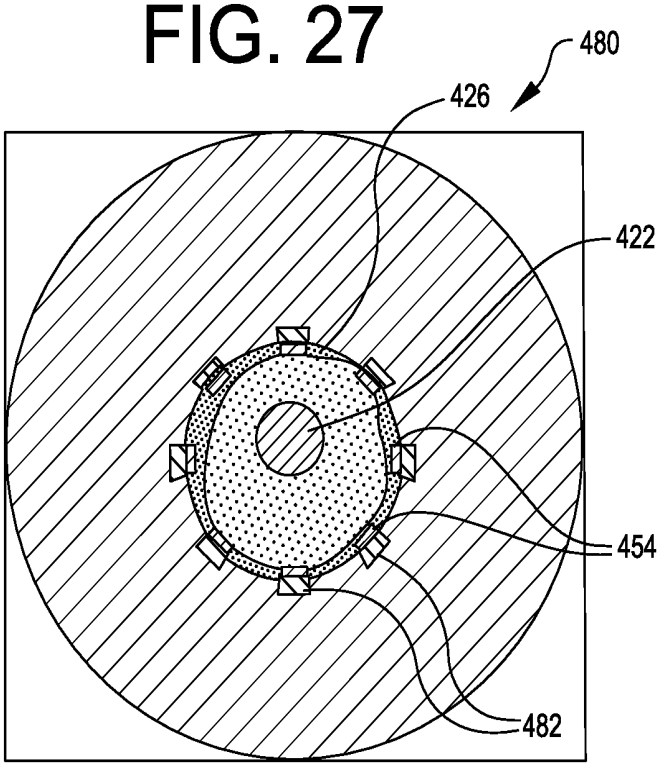

FIG. 28

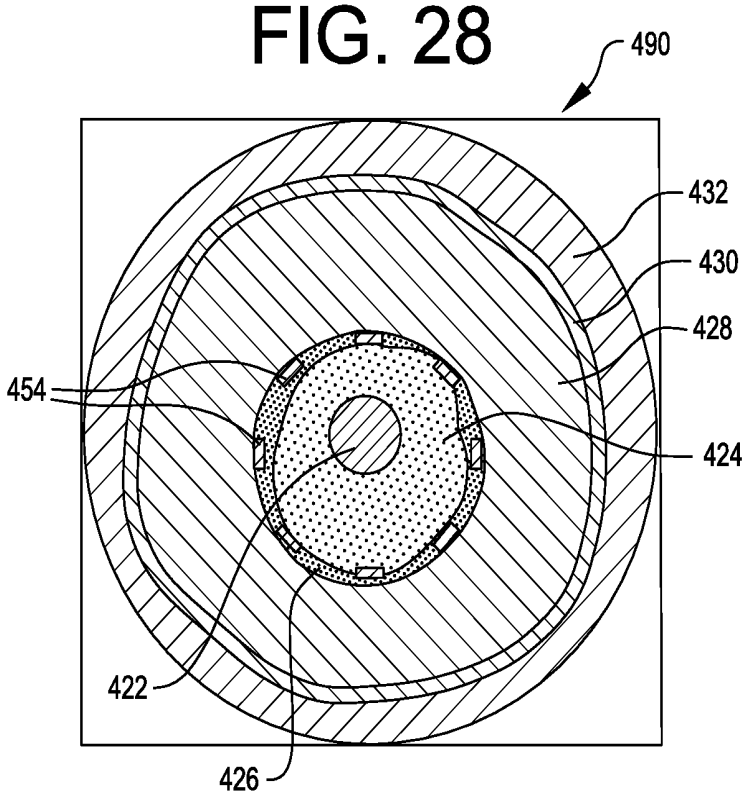

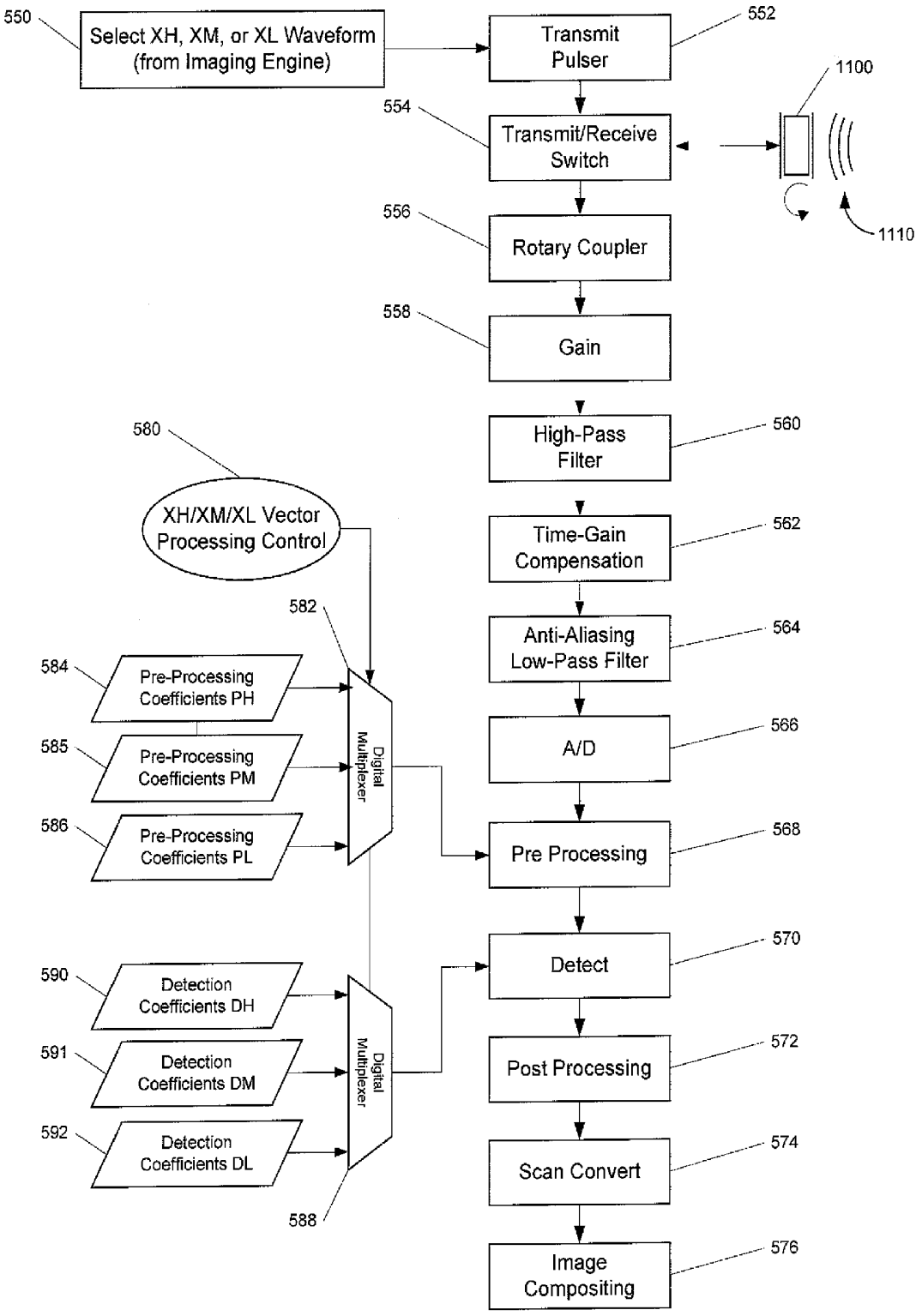
550
Select XH, XM, or XL Waveform (from Imaging Engine)
552
Transmit Pulser
1100
554
Transmit/Receive Switch
1110
556
Rotary Coupler
558
Gain
580
XH/XM/XL Vector Processing Control
560
High-Pass Filter
562
Time-Gain Compensation
564
Anti-Aliasing Low-Pass Filter
566
A/D
582
584
Pre-Processing Coefficients PH
585
Pre-Processing Coefficients PM
586
Pre-Processing Coefficients PL
Digital Multiplexer
568
Pre Processing
570
Detect
590
Detection Coefficients DH
591
Detection Coefficients DM
592
Detection Coefficients DL
Digital Multiplexer
588
572
Post Processing
574
Scan Convert
576
Image Compositing

FIG. 29

INTRAVASCULAR ULTRASOUND SYSTEM FOR CO-REGISTERED IMAGING

PRIORITY CLAIM

The present application claims the benefit of U.S. Provisional Patent Application Ser. No. 61/250,781, filed Oct. 12, 2009; the present application also claims the benefit of U.S. Provisional Patent Application Ser. No. 61/256,543, filed Oct. 30, 2009, all of the foregoing applications are incorporated herein by reference in their entireties.

BACKGROUND

The present invention generally relates to intravascular ultrasound (IVUS) imaging. The present invention more specifically relates to IVUS systems for co-registered imaging.

Intravascular ultrasound imaging is generally performed to guide and assess percutaneous coronary interventions, typically the placement of a bare-metal or drug-eluting stent. Other applications of IVUS imaging comprise further assessment of coronary artery disease.

Coronary stents generally have struts made of a metal, such as stainless steel or a cobalt chromium alloy. The metal stent struts provide a substantially larger reflected ultrasound signal than blood and soft tissue, such as neotissue grown over stent struts. The ability to detect and measure neotissue growth is particularly relevant for evaluating the stent healing process. Current commercially available IVUS systems have limited ability to detect early neotissue growth, because of a limited detectable range of reflected ultrasound signals.

Atherosclerotic lesions that are prone to rupture, so called vulnerable plaques, are of increasing interest to interventional cardiologists. One type of vulnerable plaque thought to be responsible for a large percentage of plaque ruptures is a thin-cap fibroatheroma wherein a thin (<65 μm) fibrous cap overlies a mechanically unstable lipid-rich or necrotic core. Current commercially available IVUS systems operate up to only 40 MHz and have axial resolutions that are limited to approximately 100 μm. Consequently, current commercially available IVUS systems cannot reliably detect vulnerable plaques.

It is generally necessary to increase the imaging frequency in order to improve spatial resolution. However, increased imaging frequency also leads to reduced contrast between blood and non-blood tissue that in turn makes difficult segmentation of the blood-filled lumen from the intimal plaque. Some automatic segmentation algorithms exploit the frequency-dependent ultrasound properties of blood and non-blood tissues as described for example in U.S. Pat. No. 5,876,343 by Teo. Real-time, automatic segmentation tools are often prone to errors which reduce their utility in clinical practice.

Multi-frequency imaging has been developed for transthoracic echocardiographic applications. U.S. Pat. No. 6,139,501 by Roundhill et al. describes a system that simultaneously displays two B-mode images of different imaging frequencies and bandwidths. However, this technique uses both fundamental and harmonic imaging techniques and relies upon non-linear propagation properties of tissue. Although harmonic imaging can potentially provide better spatial resolution, harmonic imaging performance in the near-field is limited. Further, harmonic IVUS imaging has not been found to be practically useful.

Multi-frequency IVUS imaging can also be achieved by use of multiple transducer imaging catheters. However, multiple transducers add complexity and cost to the disposable imaging catheter and the imaging system. The potential need to co-register the images from the separate transducers further complicates their practical use.

There exists a need for a technology that provides sufficient contrast resolution to guide percutaneous coronary interventions and sufficient contrast and spatial resolution to detect stent healing and vulnerable plaques. Further, it is desirable that such a technology does not require any co-registration step between multiple images. Still further, it is desirable that such a technology does not substantially increase system and catheter complexity and cost over existing commercial systems and catheters.

SUMMARY

The invention provides an intravascular ultrasound imaging system comprising a catheter having an elongated body having a distal end and an imaging core arranged to be inserted into the elongated body. The imaging core is arranged to transmit ultrasonic energy pulses and to receive reflected ultrasonic energy pulses. The system further comprises an imaging engine coupled to the imaging core and arranged to provide the imaging core with energy pulses to cause the imaging core to transmit the ultrasonic energy pulses. The energy pulses are arranged in repeated sequences and the energy pulses of each sequence have varying characteristics.

Each sequence of energy pulses may include at least two pulses, as for example, three pulses. The varying characteristic may be pulse energy, frequency, or bandwidth.

The imaging engine may include a processor that processes the reflected ultrasonic energy pulses in image frames and a detector that detects the varying characteristic in the reflected ultrasonic energy pulses. The imaging engine processes the frames according to the detected varying characteristic.

The imaging engine may be arranged to process only reflected ultrasonic energy pulses having a common detected characteristic. The imaging engine may be further arranged to provide a composite image based upon the varying characteristics of the sequences of reflected ultrasonic energy pulses.

The imaging engine may include a processor that processes the reflected ultrasonic energy pulses in separate image frames, each image frame corresponding to each different energy pulse characteristic and the imaging engine may provide display signals for simultaneously displaying the separate image frames.

The invention further provides a method comprising providing a catheter having an elongated body having a distal end and an imaging core arranged to be inserted into the elongated body, the imaging core being arranged to transmit ultrasonic energy pulses and to receive reflected ultrasonic energy pulses. The method further includes the step of providing the imaging core with energy pulses to cause the imaging core to transmit the ultrasonic energy pulses, wherein the energy pulses are arranged in repeated sequences and wherein the energy pulses of each sequence have varying characteristics.

BRIEF DESCRIPTION OF THE DRAWINGS

The invention, together with further features and advantages thereof, may best be understood by making reference

to the following descriptions taken in conjunction with the accompanying drawings, in the several figures of which like reference numerals identify identical elements, and wherein:

FIG. **1** is a high-level diagram of an IVUS system;

FIG. **2***a* is a block diagram of signal processing paths of an IVUS system for co-registered imaging;

FIG. **2***b* is another block diagram of signal processing paths of an IVUS system for co-registered imaging;

FIGS. **3***a* and **3***b* illustrate a time-domain signal and power spectrum, respectively, of short-time pulses;

FIG. **4***a* illustrates a pass band of a broadband power spectrum;

FIG. **4***b* illustrates another pass band of a broadband power spectrum;

FIG. **5***a* is a block diagram of an imaging engine;

FIG. **5***b* is another block diagram of an imaging engine;

FIG. **5***c* is still another block diagram of an imaging engine;

FIGS. **6***a*-**6***d* illustrate first, second, third, and fourth representative transmit pulse sequences, respectively;

FIG. **7** is a block diagram of signal processing paths of an IVUS system for co-registered imaging;

FIG. **8** is a block diagram of signal processing steps for calculation of an integrated backscatter parameter;

FIG. **9** illustrates a display comprising multiple co-registered images;

FIGS. **10***a* and **10***b* illustrate feature mapping between co-registered images;

FIG. **11** is a high-level diagram of an IVUS system;

FIG. **12** is a block diagram of a further imaging engine;

FIGS. **13**-**17** are block diagrams of digital signal processing engines;

FIG. **18** is a block diagram of the signal processing path of an IVUS system for co-registered imaging;

FIG. **19** is a cross-sectional view of a stenosed coronary artery;

FIG. **20** is a cross-sectional view of a coronary artery with an implanted stent;

FIG. **21** shows a transverse IVUS image of a stented coronary artery acquired using a high-transmit energy pulse;

FIG. **22** illustrates a repeating high-energy, medium-energy, and low-energy transmit pulse sequence;

FIG. **23** shows a transverse IVUS image of a stented coronary artery acquired using a medium-transmit energy pulse;

FIG. **24** shows a transverse IVUS image of a stented coronary artery acquired using a low-transmit energy pulse;

FIG. **25** shows a transverse IVUS image with a selected dynamic range of a stented coronary artery acquired using a high-transmit energy pulse;

FIG. **26** shows a transverse IVUS image with a selected dynamic range of a stented coronary artery acquired using a medium-transmit energy pulse;

FIG. **27** shows the stent regions of a transverse IVUS image with a selected dynamic range of a stented coronary artery acquired using a low-transmit energy pulse;

FIG. **28** shows a composite image of a high-transmit energy transverse IVUS image of a stented coronary artery, a medium-transmit energy transverse IVUS image of a stented coronary artery, and a low-transmit energy transverse IVUS image of a stented coronary artery; and

FIG. **29** is a flow diagram of the signal processing path of an IVUS system for imaging with a high-transmit, medium-transmit and low-transmit energy pulse sequence.

DETAILED DESCRIPTION OF THE EMBODIMENTS

FIG. **1** is a high-level block diagram of an IVUS system comprised of an IVUS imaging catheter **1000**, a patient interface module **2000**, and an imaging engine **3100**. The catheter is typically delivered to a coronary artery via a transfemoral or transradial retrograde route. The imaging catheter **1000** is coupled mechanically and electrically to the patient interface module **2000**. The imaging engine **3100** is used to control operation of the patient interface module **2000** and catheter **1000** for purposes of coronary artery imaging. The following descriptions of an IVUS imaging catheter are directed to the case of a mechanically rotating imaging core. Each IVUS image comprises a pre-determined number of vectors (or scan lines) and samples per vector. Most currently available commercial IVUS systems utilize 256 vectors per image. The number of samples per vector varies generally between approximately 256 and 2048 samples for commercially available IVUS systems and depends in part on imaging frequency and data type (e.g., RF or baseband).

FIG. **2***a* is a block diagram of one embodiment of signal processing paths of an IVUS system for co-registered imaging. A waveform is selected in step **102**, generally within the imaging engine. A transmit waveform is then generated by a transmit pulser in step **104** that is generally located in the patient interface module. The transmit waveform is sent through a transmit/receive (T/R) switch in step **106** to an ultrasound transducer **1100**. The transducer may operate over frequency ranges of 10 MHz to 80 MHz, generally between 20 MHz and 60 MHz for intracoronary imaging.

The transducer emits an ultrasonic pressure field **1110** to insonify the coronary artery. Some ultrasonic energy is backscattered and received by the transducer. The received ultrasound passes through the T/R switch in step **106** and a rotary coupler in step **108**. The rotary coupler may be an inductive rotary coupler or a liquid metal rotary coupler. Alternatively, the rotary coupler may be a rotary capacitive coupler as described, for example, in co-pending U.S. patent application Ser. No. 12/465,853 filed May 14, 2009, in the names of Silicon Valley Medical Instruments, Inc. and titled IVUS System with Rotary Capacitive Coupling, which application is hereby incorporated herein by reference in its entirety. The rotary coupler interfaces the mechanically rotating imaging core of the catheter to the non-rotating electronics of the patient interface module.

The received signal then passes through a gain amplifier in step **109**, a high-pass filter in step **110**, and a time-gain compensation amplifier in step **112**. The time-gain compensation is provided, because of the increased attenuation of the ultrasound signal as the signal propagates further into the coronary artery. The signal is next sent through an anti-aliasing low-pass filter in step **114** before digitization in step **116**.

The digitized signals are then processed according to multi-frequency techniques comprising a low-frequency path **120** and a high-frequency path **130**. The low-frequency and high-frequency processing paths comprise similar processing stages that may differ due to imaging parameters such as pass band, field of view, and signal-to-noise ratio.

Referring now to FIGS. **3** and **4**, the time-domain response **202** and power spectrum **204** are respectively shown in FIGS. **3***a* and **3***b* for a short-time pulse of a 60 MHz IVUS imaging transducer having a fractional bandwidth >60%. An important aspect of the present invention is the use of transducers with large fractional bandwidths, generally >50% fractional bandwidth. Transducers having fractional bandwidths <50% may also be used, but the use of such transducers is expected to be less effective with reduced utility. Another important aspect of the present invention is the use of transducers with uniformly high

sensitivities across the useful bandwidths. The selected low and high frequencies may comprise overlapping bandwidths **222**, **224** or non-overlapping bandwidths **226**, **228** with corresponding pass band center frequencies F**1**, F**2** as illustrated respectively in FIGS. **4***a* and **4***b*. A potential benefit of the use of overlapping bandwidths is that wider bandwidths generate images having better spatial resolution. In one embodiment of the present invention, the low pass band center frequency F**1** is 40 MHz, the high pass band center frequency F**2** is 60 MHz, the low pass band **222** is 30 MHz to 50 MHz, and the high pass band **224** is 45 MHz to 75 MHz. In another embodiment of the present invention, the catheter comprises a broadband 40 MHz transducer, the low pass band center frequency is 30 MHz, and the high pass band center frequency is 50 MHz. In still another embodiment of the present invention, the catheter comprises a broadband 35 MHz transducer, the low pass band center frequency is 25 MHz, and the high pass band center frequency is 40 MHz.

Referring again to FIG. **2***a*, the low-frequency path digitized data are first pre-processed in step **122**. Pre-processing, as known in the art, may generally comprise bandpass filtering and vector processing techniques. The envelope of the pre-processed data is detected in step **124** followed by post-processing in step **126**. Post-processing generally comprises logarithmic compression and gamma correction to generate a visually appealing and useful image. The post-processed data are then scan converted in step **128** from polar coordinates to Cartesian coordinates. Pre-processing, detection, post-processing, and scan conversion are signal and image processing techniques known to those skilled in the art of medical ultrasound imaging.

The high-frequency path digitized data are processed in an analogous manner. The high-frequency path digitized data are first pre-processed in step **132**. Pre-processing, again, generally comprises bandpass filtering and vector processing. The envelope of the pre-processed data is detected in step **134** followed by post-processing in step **136**. Post-processing generally comprises logarithmic compression and gamma correction to generate a visually appealing and useful image. The post-processed data are then scan converted in step **138** from polar coordinates to Cartesian coordinates.

The low-frequency and high-frequency scan-converted images **152**, **154** are then simultaneously displayed in step **150**. A low-frequency image comprises better contrast between blood and non-blood tissues to facilitate lumen border detection. A high-frequency image comprises better spatial resolution of lesion features such as thin fibrous caps. The low-frequency and high-frequency scan-converted images **152**,**154** are co-registered, because the same ultrasound data are used to generate both images.

The signal processing paths illustrated in FIG. **2***a* can be implemented in numerous physical configurations. An important aspect of the present invention is the physical configuration of the imaging engine. FIG. **5***a* is a block diagram for one embodiment of the imaging engine **3100** comprising a single board computer **3102**, a dedicated digital signal processing (DSP) module **3120**, and an interface board **3180**. The DSP module **3120** is used to select the transmit waveform **3182** to be sent to the patient interface module. The time-gain compensation amplifier **3184** and anti-aliasing low-pass filter **3186** are located on the interface board **3180**. The analog-to-digital converter (or digitizer) **3128** is located in the DSP module **3120**. The DSP module **3120** may further comprise a field-programmable gate array (FPGA) **3122**. The low-frequency signal and high-frequency signal processing paths **120**,**130** illustrated in FIG. **2***a* are generally implemented in the FPGA. An important aspect of this embodiment is that the co-registered imaging is performed by an imaging engine comprising a single analog-to-digital converter and a single FPGA.

FIG. **5***b* is a block diagram of another embodiment of the imaging engine of the present invention comprising a first DSP module **3120** and a second DSP module **3140** wherein a single analog-to-digital converter (or digitizer) **3128** and two FPGAs **3122**, **3142** are available. The addition of a second DSP module comprising an FPGA provides increased computational processing power at the expense of increased device complexity and cost. The same digitized data are processed by both FPGAs.

FIG. **5***c* is a block diagram of still another embodiment of the imaging engine of the present invention comprising a first DSP module **3120** and a second DSP module **3140** wherein two analog-to-digital converters (or digitizers) **3128**, **3148** and two FPGAs **3122**, **3142** are available. A sampling clock **3126** synchronizes both digitizers **3128**, **3148**. The embodiment of the 2 digitizer/2 FPGA imaging engine further comprises a second time-gain compensation amplifier **3188** and second anti-aliasing low-pass filter **3190**. The addition of a second digitizer **3148**, time-gain compensation amplifier **3188**, low-pass filter **3190** provides increased computational processing power and flexibility at the expense of increased device complexity. The added flexibility enables compensation for differing attenuation of the ultrasound pressure wave through the tissue resulting from the different frequency bands.

FIG. **2***b* is a block diagram of another embodiment of signal processing paths of an IVUS system for co-registered imaging comprising an embodiment of the imaging engine illustrated in FIG. **5***c*. The signal scattered back from the tissue is received by the transducer **1100** and then passes through a transmit/receive switch in step **106**, a rotary coupler in step **108**, a gain amplifier in step **109**, and a high-pass filter in step **110**. The high-pass filtered signals are then processed according to multi-frequency techniques comprising a low-frequency processing path **120**A and a high-frequency processing path **130**A. The low-frequency processing path **120**A and high-frequency processing path **130**A include similar processing stages that may differ due to imaging parameters such as pass band, field of view, and signal-to-noise ratio. Time-gain compensation in step **112** is first applied to the low-frequency path signal. Time-gain compensation is provided, because of the increased attenuation of the ultrasound signal as the signal propagates further into the coronary artery. The TGC-amplified low-frequency path signal is next sent through an anti-aliasing low-pass filter in step **114** before analog-to-digital (A/D) conversion (or digitization) in step **116**. The low-frequency path digitized data are first pre-processed in step **122**. Pre-processing generally comprises bandpass filtering and vector processing techniques. The envelope of the pre-processed data is detected in step **124** followed by post-processing in step **126**. Post-processing generally comprises logarithmic compression and gamma correction to generate a visually appealing and useful image. The post-processed data are then scan converted in step **128** from polar coordinates to Cartesian coordinates.

The high-frequency path **130**A signals are processed in an analogous manner. Time-gain compensation in step **112**A, anti-aliasing low-pass filter in step **114**A, and A/D conversion in step **116**A occur first after high-pass filtering in step **110**. The high-frequency digitized data are then pre-processed in step **132**. Pre-processing generally comprises

bandpass filtering and vector processing. The envelope of the pre-processed data is detected in step **134** followed by post-processing in step **136**. Post-processing generally comprises logarithmic compression and gamma correction to generate a visually appealing and useful image. The post-processed data are then scan converted in step **138** from polar coordinates to Cartesian coordinates. The low-frequency and high-frequency scan-converted images **152**, **154** are then simultaneously displayed in step **150**. The multi-frequency signal processing paths split after high-pass filtering in step **110** in the embodiment of the signal processing paths shown in FIG. **2***b* whereas the multi-frequency signal processing paths split after A/D conversion in step **116** in the embodiment of the signal processing paths shown in FIG. **2***a*. The split of the multi-frequency signal processing paths after high-pass filtering provides for time-gain compensation appropriate for different imaging frequencies.

Referring now to FIGS. **6***a*-**6***d*, a series of imaging waveform sequences are illustrated. FIG. **6***a* illustrates one embodiment in which a single pulse sequence **10** comprises transmitting the same waveform Xc for each vector of an IVUS image. FIG. **6***b* illustrates another embodiment comprising a pulse sequence **20** of alternating low-frequency X**1** and high-frequency X**2** waveforms. A potential advantage of an alternating pulse sequence over a single pulse sequence is that the transmitted energy can be increased or decreased for the selected pass bands of the multi-frequency processing. The ability to adjust transmit energy may benefit image quality of co-registered images that are simultaneously displayed. FIG. **6***c* illustrates still another embodiment comprising a pulse sequence **30** of alternating imaging Xi and parametric imaging Xp waveforms. The imaging waveform Xi may include a Xc, X**1**, or X**2** waveform. The parametric imaging waveform Xp is selected to optimize analysis of at least one ultrasound tissue classification parameter including integrated backscatter, attenuation, strain, and motion. The use of a more narrowband waveform may provide benefit to correlation-based or Doppler-based motion analysis. FIG. **6***d* illustrates still yet another embodiment including a pulse sequence **40** of alternating imaging and parametric imaging waveforms Xi, Xp wherein multiple parametric imaging waveforms Xp are transmitted between imaging waveforms Xi. The use of repeated pulses may provide additional benefits for signal-to-noise conditions.

Thus, as may be seen from the above, and in accordance with aspects of the present invention, an imaging engine coupled to an imaging core may be arranged to provide the imaging core with energy pulses to cause the imaging core to transmit ultrasonic energy pulses. The energy pulses may be arranged in repeated sequences and the energy pulses of each sequence may have varying characteristics. For example, each sequence of energy pulses may include at least two pulses. Also, the varying characteristic may be pulse energy.

FIG. **7** shows a block diagram of one embodiment of signal processing paths of an IVUS system for co-registered imaging wherein the co-registered images include a grayscale image **182** and a parametric image **184**. The parametric image **184** may include a multi-parametric image. The transmit waveform selected in step **102** and sent from the imaging engine may include a single pulse sequence **10** or an imaging and parametric imaging pulse sequence **30** as illustrated in FIGS. **6***a* and **6***c*. The signal processing path to the digitization step **116** is similar to the signal processing path for the multi-frequency imaging illustrated in FIG. **2***a*.

The digitized signals are then processed according to a grayscale imaging path **160** and a parametric imaging path **170**. The grayscale imaging path digitized data are first pre-processed in step **162**. Pre-processing generally comprises bandpass filtering and vector processing techniques. The envelope of the pre-processed data is detected in step **164** followed by post-processing in step **166**. Post-processing generally comprises logarithmic compression and gamma correction to generate a visually appealing and useful image. The post-processed data are then scan converted in step **168** from polar coordinates to Cartesian coordinates.

The processing stages of the parametric imaging path **170** include a pre-processing step **172**, a parametric analysis step **174**, a post-processing step **176**, and a scan conversion step **178**. The particular details of each parametric imaging processing step depend upon the at least one parameter to be calculated.

In one embodiment of the present invention a parametric image of integrated backscatter is generated. The integrated backscatter pre-processing step **172** comprises bandpass filtering and vector processing techniques. The filter pass band may be determined from the −3 dB bandwidth of the transducer. The integrated backscatter parametric analysis in step **174** may include a sliding window technique. Sliding window techniques are known to those skilled in the art of ultrasound tissue characterization.

Referring now to FIG. **8**, a block diagram illustrates one embodiment of the signal processing stages for calculation of the integrated backscatter parameter using a sliding window technique. A region of interest (ROI) of the pre-processed data **500** is first selected in step **502**. A time-domain window such as a Hamming or Hann window may be applied to each vector of the ROI to minimize edge discontinuities in Fast Fourier Transform (FFT) spectral analysis at the cost of reduced frequency resolution. The ROI comprises a pre-determined number of vectors and vector samples. The number of vectors and vector samples depends upon details including vector density, sample rate, optimal ROI size, and signal-to-noise metrics.

In one embodiment of the present invention the system provides a vector density of 1024 vectors per IVUS image and a sample rate of 400×10^6 samples/s. An optimal ROI size balances a minimal radial extent of the ROI with a maximal signal-to-noise ratio. A lateral extent of the ROI comparable to the radial extent can facilitate subsequent parametric image analysis. Multiple vectors also permit signal averaging. Further, the selected ROI size may be range dependent, because the physical vector spacing increases with range. An ROI size of 7 vectors and 32 samples at a range of 1.5 mm provides a ROI that is approximately 60 μm×60 μm. This size may be suitable for small-scale atherosclerotic lesion features such as thin-fibrous caps.

The average power spectrum is calculated in step **504** for the ROI by calculating the power spectrum of each vector and then averaging. The power spectrum is calculated generally using FFT techniques. Averaging is performed generally in the logarithmic (dB) domain, but may be performed in the linear domain. The average power spectrum may then be compensated for system and transducer effects in step **506** comprising range-dependent sensitivity and frequency-dependent transducer sensitivity. The integrated backscatter parameter is calculated in step **508** by summing the compensated, average power spectrum values of the selected bandwidth and dividing by said selected bandwidth. Additional ROIs are selected by sliding the window (or ROI) over the pre-processed data **500** or pre-defined subset of the pre-processed data. The degree of overlap of ROIs is

selected to balance smoothing in the parametric image by maximizing overlap with computational cost by minimizing overlap. For a ROI size of 7 vectors×32 samples, the sliding window overlap generally comprises between 16 samples (or 50%) and 24 samples (or 75%) along a vector and between 4 vectors (or approximately 50%) and 6 vectors (or approximately 85%) across vectors. The integrated backscatter parametric data are sent to the post-processing step **176** (of FIG. **7**) when there are no more ROIs remaining to be analyzed.

Post-processing in step **176** of the integrated backscatter image includes thresholding and gamma correction. In one embodiment of the present invention, the integrated backscatter image is thresholded to display lipid-rich ROIs which are known to have relatively low integrated backscatter values. In alternative embodiments, the integrated backscatter image is thresholded at multiple levels to distinguish multiple tissue types. The post-processed integrated backscatter image is then scan converted in step **178**.

The scan-converted grayscale image and scan-converted integrated backscatter parametric image are then simultaneously displayed in step **180**. A grayscale image may provide better structural detail. An integrated backscatter parametric image may provide better plaque composition detail. Further, the grayscale and integrated backscatter parametric images **182**,**184** are co-registered, because the same ultrasound data are used to generate both images.

FIG. **9** illustrates a display **190** comprising four co-registered images **192**, **194**, **196**, **198**. The four co-registered images may comprise at least one grayscale image and at least one parametric image. In one embodiment of the present invention, the display comprises a 40 MHz grayscale image, a 60 MHz grayscale image, and an integrated backscatter parametric image.

The present invention facilitates mapping of image features between co-registered images. IVUS images of lower ultrasound frequencies generally provide better contrast between blood and non-blood tissues whereas IVUS images of higher ultrasound frequencies generally provide better spatial resolution of atherosclerotic lesions. FIG. **10***a* illustrates a first IVUS image **300** of lower frequency and second IVUS image **320** of higher frequency. Catheter masks **302**, **322** represent catheter position relative to a coronary artery section. A lumen contour **308** identified in the first image **300** can be mapped **312** to a lumen contour **328** in the second image **320**. The lumen contour segments blood **304** from non-blood tissues. A vessel contour **310** identified in the first image **300** can be mapped **314** to a vessel contour **330** in the second image **320**. The lumen and vessel contours **308**, **310** segment atherosclerotic plaque **306** from other tissues. The mapped contours **328**, **330** of the higher-frequency IVUS image enable further processing of the atherosclerotic plaque.

FIG. **10***b* illustrates mapping features more prominent in a first image **340** to a second image **360** and mapping features more prominent in said second image **360** to said first image **340**. The first image may comprise a grayscale image, and the second image may comprise a parametric image. A lumen contour **348** in the first image **340** is mapped **352** to a lumen contour **368** in the second image **360**. A vessel contour **370** and ROI **372** in the second image **360** are respectively mapped **374**, **376** to a second vessel contour **350** and second ROI **352** in the first image **340**.

It is desirable that the present invention provide optimal imaging performance and computational efficiency with minimal device complexity. FIG. **11** shows a high-level diagram of one embodiment of an IVUS system for co-registered imaging. The following descriptions of an IVUS system for co-registered imaging are directed to the case of an IVUS system for display of two co-registered grayscale images. The IVUS system comprises two images **3802**, **3803**, an imaging engine **3804**, a patient interface module (PIM) **2000**, and an IVUS imaging catheter **1000**. The following descriptions of the IVUS imaging catheter **1000** are directed at the case of a mechanically rotating imaging core. The imaging engine **3804** comprises a display engine **3806**, a DSP engine **3808**, transmit (Tx) logic **3810**, a transmit buffer **3812**, a receive (Rx) signal conditioning stage **3814**, and an analog-to-digital converter (ADC) **3816**.

The DSP engine **3808** provides computing power for real-time, simultaneous co-registered imaging. The DSP engine **3808** sends control signals to the transmit logic **3810** that generates an analog transmit pulse sequence. The transmit pulse passes through the transmit buffer **3812** before going to the PIM **2000**. The PIM **2000** is the interface between the catheter **1000** and the imaging engine **3804**. The PIM **2000** provides for transmitting transducer excitation energy, receiving transducer signal returns, and sending signal returns to the imaging engine **3804**. The return signals pass through a receive signal conditioning stage **3814** and analog-to-digital converter **3816**. The digitized return signals are then processed in the DSP engine **3808**. Image data are sent to the display engine **3806** and streamed for real-time simultaneous display of co-registered images **3802**, **3803**.

FIG. **12** illustrates one embodiment of a physical configuration of the imaging engine **3100**. The imaging engine **3100** performs all image generation, display, and control of the entire system. The imaging engine **3100** may include a general processing unit **3500**, a DSP module **3600**, and an interface board **3700**.

The general processing unit **3500** may include a central processing unit (CPU) **3502**, a memory controller **3504**, dynamic random access memory (DRAM) **3506**, a digital bus interface **3508**, and a peripheral controller **3510**. The DSP module **3600** may include a DSP engine **3610**, transmit logic circuitry **3612**, a digital-to-analog converter (DAC) **3620**, an analog-to-digital converter (ADC) **3630**, and a sampling clock **3640**. A high-speed digital bus **3512** connects the digital bus interface **3508** to the DSP engine **3610**. The interface board **3700** may include a transmit buffer **3702**, a time gain compensation (TGC) amplifier **3704**, and an anti-aliasing low-pass filter (LPF) **3706**.

The DSP engine **3610** controls the transmit logic circuitry **3612** to send an analog transmit signal to the transmit buffer **3702**. The analog transmit signal may include a pulse wherein the pulse may include at least one rectangular pulse. The analog transmit signal is sent from the interface board **3700** to the PIM. The DSP engine **3610** further generates a digital TGC signal that is converted by the DAC **3620** to an analog TGC signal. The analog TGC signal provides the level of TGC amplification **3704** applied to signals received from the PIM. The low-pass filter **3706** minimizes aliasing in the TGC-amplified signals.

The anti-aliased TGC-amplified return signals are digitized and then processed by the DSP engine **3610** for co-registered imaging. A sampling clock **3640** synchronizes the ADC (or digitizer) **3630** and DSP engine **3610**. Co-registered images are streamed from the DSP engine **3610** to the general processing unit **3500** for display of images.

Referring now to FIGS. **13-17**, the DSP engine **3610** may include different forms of signal processors. FIGS. **13-15** show diagrams of a DSP engine **3610** including a field-programmable gate array (FPGA) **3902**, a DSP chip **3904**

and random-access memory (RAM) **3906**, or an application-specific integrated circuit (ASIC) **3908**. The DSP engine may further include multiple signal processors. FIG. **16** shows a diagram of a DSP engine **3610** that includes a first FPGA **3910** and a second FPGA **3912**. FIG. **17** shows a diagram of a DSP engine **3610** that includes a massively parallel processor array (MPPA) **3914** of CPUs and RAM modules. The most cost effective and computationally efficient signal processor will depend on the specific application. Field-programmable gate arrays are commonly used in IVUS imaging systems.

FIG. **18** illustrates a signal processing path for co-registered multi-frequency imaging that provides for optimizing co-registered grayscale imaging performance while minimizing device cost and complexity. The following descriptions are directed at the case of an alternating transmit pulse sequence **20** as illustrated in FIG. **6***b* wherein a first pulse sequence X**1** has a lower imaging frequency and a second pulse sequence X**2** has a higher imaging frequency. A potential advantage of the alternating pulse sequence **20** over a single pulse sequence **10** shown in FIG. **6***a* is that the transmitted energy can be increased or decreased for the selected pass bands of the multi-frequency processing. The ability to adjust transmit energy may benefit image quality of co-registered images that are simultaneously displayed.

The received signal is converted from analog to digital (A/D) in step **300**. The digitized signals are pre-processed in step **302** wherein pre-processing generally includes band-pass filtering and vector processing techniques. The specific form of pre-processing depends on whether the transmit signal is an X**1** pulse or X**2** pulse. A digital multiplexer **330** receives a first set of pre-processing coefficients **332** and a second set of pre-processing coefficients **334**. The pre-processing coefficients include filter coefficients for band-pass filtering. A vector processing control **320** determines which set of pre-processing coefficients to use for pre-processing. The envelope of the pre-processed signal is detected in step **304**. The vector processing control **320** determines whether a digital multiplexer **340** selects a first set of detection coefficients **342** or a second set of detection coefficients **344** for detection processing. The detected signal is then post-processed in step **306** wherein post-processing generally comprises logarithmic compression and gamma correction to generate a visually appealing and useful image. The post-processed signals are then scan converted in step **308** from polar coordinates to Cartesian coordinates.

The low-frequency and high-frequency scan-converted images **312**, **314** are then simultaneously displayed in step **310**. A low-frequency image may provide better contrast between blood and non-blood tissues to facilitate lumen border detection. A high-frequency image may provide better spatial resolution of lesion features. The low-frequency and high-frequency scan-converted images **312**,**314** are co-registered, because both sets of image data are acquired at substantially the same time when using alternating transmit pulse sequences.

In another embodiment, the alternating transmit pulse sequence may include alternating groups of pulses. A pulse sequence may include alternating groups of X**1** and X**2** pulse sequences wherein each group of X**1** and X**2** pulses includes at least two (2) pulses. The temporal delay will be larger between acquisitions of the X**1** and X**2** images, but there may be advantages to fewer alternations between X**1** and X**2** pulse sequences.

A key advantage of the signal processing path illustrated in FIG. **18** is that only one digitizer is required. Further, the digital signal processing can be performed in a single FPGA. Still further, the multi-frequency processing can be performed without duplication of signal processing stages.

An important aspect of the present invention is the use of an IVUS system for co-registered imaging comprising an imaging engine, a patient interface module, and an IVUS catheter. The imaging engine may comprise a general processing unit, a DSP module, and an interface board. The DSP module comprises an analog-to-digital converter and a DSP engine. The DSP engine may comprise a FPGA, DSP chip, or ASIC. The DSP engine may alternatively comprise multiple FPGAs or a massively parallel processing array of CPUs and RAM modules. Another important aspect of the present invention is the use of an IVUS catheter comprising a broadband (>50% fractional bandwidth) ultrasound transducer with high sensitivity wherein both a low pass band and a high pass band can be used to generate grayscale images. Low pass band and high pass band center frequencies may respectively comprise 40 MHz and 60 MHz, 30 MHz and 50 MHz, 25 MHz and 40 MHz, and other combinations with different frequency spacing. Still another important aspect of the present invention is the use of a programmable transmit pulse sequence. The transmit pulse sequence may comprise a single pulse imaging sequence, an alternating low-frequency and high-frequency imaging sequence, or an alternating imaging and parametric imaging sequence. Still yet another important aspect of the present invention is the display of at least two (2) co-registered images comprising at least one grayscale image. The co-registered images may further comprise at least one parametric image. A further important aspect of the present invention is the mapping of image features between co-registered images wherein image features comprise contours and regions of interest.

It is also desirable to provide improved contrast resolution for imaging of coronary arteries having implanted stents. The ability to detect and measure stent healing, or early neotissue growth over coronary stent struts, is of particular relevance. FIG. **19** shows an illustration of a cross-section of a stenosed coronary artery **400**. The coronary artery includes a blood-filled lumen **402**, an intimal plaque layer **404**, a medial layer **406**, and an adventitial layer **408**. The lumen generally has a cross-sectional area less than 4 mm^2. FIG. **20** shows an illustration of the same coronary artery **400** as in FIG. **19** after stent implantation. The stent struts **410** are positioned in proximity to the lumen-plaque border. The stent provides for an increased lumen cross-sectional area to enable improved blood flow through the artery.

FIG. **21** shows a transverse IVUS image **420** of a stented coronary artery acquired with a high-transmit energy pulse having an amplitude generally greater than 50 V. The transverse IVUS image **420** includes a catheter mask **422** to indicate position of the IVUS catheter relative to the coronary artery. The IVUS image **420** further shows ultrasound reflections from a blood-filled lumen **424**, neotissue growth **426**, an intimal plaque layer **428**, a medial layer **430**, and an adventitial layer **432**. The neotissue growth **426** is a result of the stent healing process. Uncovered struts of drug-eluting stents are considered a factor in the adverse event of late stent thrombosis. The transverse IVUS image **420** still further includes substantially strong ultrasound reflections from the stent struts **434** as well as so-called stent blooming artifacts **436**. The stent blooming artifacts can result from saturation of the receive-side electronics that are part of the IVUS system and characteristically appear on the side of the stent struts **434** away from the catheter mask **422**. The combined thickness of the stent reflection **434** and stent blooming artifact **436** is generally substantially larger than

the physical thickness of the stent struts, which is approximately 100 microns or smaller. The stent blooming artifacts **436** degrade image quality.

Stent blooming artifacts can be prevented by sufficiently decreasing the energy of the transmit pulse to avoid saturation of the receive-side electronics of the IVUS system. In one embodiment of the present invention, a three-pulse sequence that includes a high-transmit energy pulse, a medium-transmit energy pulse, and a low-transmit energy pulse may be used to visualize neotissue growth, provide adequate penetration of the ultrasound energy into the coronary artery, and prevent stent blooming artifacts. FIG. **22** illustrates a repeating pulse sequence **22** of high-energy transmit pulses XH, medium-energy transmit pulses XM, and low-energy transmit pulses XL.

The transverse IVUS image **420** shown in FIG. **21** is acquired with a high-transmit energy pulse and enables visualization of neotissue growth and penetration beyond the medial layer **430**. FIG. **23** shows a transverse IVUS image **440** of the same stented coronary artery shown in FIG. **21**, but acquired with a medium-transmit energy pulse having an amplitude less than the amplitude of the high-transmit energy pulse. The transverse IVUS image **440** includes a catheter mask **422** to indicate position of the IVUS catheter relative to the coronary artery. The IVUS image **440** further shows ultrasound reflections from a blood-filled lumen **424**, neotissue growth **426**, and an intimal plaque layer **428**. The transverse IVUS image **440** still further includes ultrasound reflections from the stent struts **442** and stent blooming artifacts **444**.

FIG. **24** shows a transverse IVUS image **450** of the same stented coronary artery shown in FIG. **21**, but acquired with a low-transmit energy pulse having an amplitude less than the amplitude of the high-transmit energy pulse. The transverse IVUS image **450** includes a catheter mask **422** to indicate position of the IVUS catheter relative to the coronary artery. The IVUS image **440** further shows ultrasound reflections from neotissue growth **426** and parts of the intimal plaque layer **428**. The transverse IVUS image **440** still further includes ultrasound reflections from the stent struts **454**. Because of the low-transmit energy level of the pulse, there will be no stent blooming artifact and more distant sections of the coronary artery such as the medial and adventitial layers may not be visualized. The low-transmit energy level of the pulse may degrade the ability to detect and visualize the small ultrasound reflections from a blood-filled lumen.

A high-transmit energy IVUS image, a medium-transmit energy IVUS image, and a low-transmit energy IVUS image can be co-registered by using a sequence of repeated high-transmit energy, medium-transmit energy and low-transmit energy pulses. Referring now to FIG. **25**, a high-transmit energy IVUS image **460** can be further processed to include deeper tissues that are visualized with a high-transmit energy pulse such as the medial layer **430** and the adventitia **432**. Referring now to FIG. **26**, a medium-transmit energy IVUS image **470** can be further processed to have sections **472** of the image that include the stents and stent blooming artifacts removed from the image. Referring now to FIG. **27**, a low-transmit energy IVUS image **480** can be further processed to include the neotissue growth **426** and only those sections **454**,**472** that map to the sections of the medium-transmit energy IVUS image **470** that include the stents and stent blooming artifacts **472**. Referring now to FIG. **28**, the further processed high-transmit energy IVUS image **460** the further processed medium-transmit energy IVUS image **470**, and the further processed low-transmit energy IVUS image **480** can be combined into a composite image **490** that visualizes neotissue growth **426** over stent struts **454**, visualizes tissue beyond and including the medial layer **430**, and avoids stent blooming artifacts.

FIG. **29** illustrates one embodiment of a signal processing path generating a composite image from images acquired using high-transmit, medium-transmit, and low-transmit energy pulses. The following descriptions are directed to the case of an transmit pulse sequence **22** as illustrated in FIG. **22** wherein a first pulse XH has a high-transmit energy, a second pulse XM has a medium-transmit energy, and a third pulse XL has a low-transmit energy.

A high-transmit energy, medium-transmit energy, or low-transmit energy waveform, generally stored within an imaging engine, is selected in step **550**. A transmit waveform is then generated by a transmit pulser in step **552**. The transmit waveform is sent through a transmit/receive (T/R) switch in step **554** to an ultrasound transducer **1100**. The transducer may operate over frequency ranges of 10 MHz to 80 MHz, generally between 20 MHz and 60 MHz for intracoronary imaging.

The transducer emits an ultrasonic pressure field **1110** to insonify the coronary artery. Some ultrasonic energy is backscattered and received by the transducer. The received ultrasound passes through the T/R switch in step **554** and a rotary coupler in step **556**. The rotary coupler may be an inductive rotary coupler or a liquid metal rotary coupler. The rotary coupler interfaces the mechanically rotating imaging core of the catheter to the non-rotating electronics of the patient interface module.

Gain is then applied to the received signal in step **558**. A high-pass filter is next applied to the amplified signal in step **560**. A time-varying gain is applied to the high-pass filtered signal in step **562**. The time-gain compensation is provided, because of the increased attenuation of the ultrasound signal as the signal propagates further into the coronary artery. An anti-aliasing low-pass filter is next applied to the signal in step **564** before the signal is digitized in step **566**.

The digitized signals are pre-processed in step **568** wherein pre-processing generally includes band-pass filtering and vector processing techniques. The specific form of pre-processing depends on whether the transmit signal is a high-transmit energy pulse XH or a low-transmit energy pulse XL. A digital multiplexer **584** receives a first set of pre-processing coefficients PH **584**, a second set of pre-processing coefficients PM **585**, and a third set of pre-processing coefficients PL **586**. The pre-processing coefficients include filter coefficients for band-pass filtering. A vector processing control **580** determines which set of pre-processing coefficients to use for pre-processing. The envelope of the pre-processed signal is detected in step **570**. The vector processing control **580** determines whether a digital multiplexer **588** selects a first set of detection coefficients DH **590**, a second set of detection coefficients DM **585**, or a third set of detection coefficients DL **592** for detection processing. The detected signal is then post-processed in step **572** wherein post-processing generally includes logarithmic compression and gamma correction to generate a visually appealing and useful image.

The post-processed signals can then be scan converted from polar coordinates to Cartesian coordinates in step **574**. The high-transmit energy, medium-transmit energy, and low-energy transmit scan-converted images are then combined into a composite image in step **576**. The combination or fusion of the three images into a single composite image are achieved by selecting a portion of the dynamic range of each individual image. The composite image may then have

a wider dynamic range than any single image. The composite image may then be compressed to satisfy parameters of the display device. The composite image includes neotissue growth over stent struts and tissue beyond and including the medial layer. The composite image further avoids stent blooming artifacts. The individual high-transmit energy, medium-transmit energy, and low-transmit energy images can be first aligned during post-processing to minimize motion artifacts. In addition, the images can be acquired during a period of relatively little motion, such as end diastole of the cardiac cycle, to further minimize motion artifacts. Motion artifacts can be further minimized by minimizing the depth or range of acquired data in order to minimize time between pulse transmissions.

While particular embodiments of the present invention have been shown and described, modifications may be made, and it is therefore intended to cover in the appended claims all such changes and modifications which fall within the true spirit and scope of the invention.

What is claimed is:

1. An intravascular ultrasound imaging system, comprising:

a catheter having an elongated body having a distal end, the catheter having an imaging core configured to be inserted into the elongated body, the imaging core being configured to transmit ultrasonic energy pulses and to receive reflected ultrasonic energy pulses; and

an imaging engine coupled to the imaging core and configured to provide the imaging core with energy pulses, the energy pulses being ultrasonic, to cause the imaging core to transmit the ultrasonic energy pulses, each energy pulse having a predefined energy pulse characteristic within a plurality of predefined energy pulse characteristics, the energy pulses being transmitted such that the associated predefined energy pulse characteristics are arranged in a repeating sequence, wherein

the imaging engine is further configured to process the reflected ultrasonic energy pulses into separate image frames, the separate image frames being acquired from the sequence of predefined energy pulse characteristics of the reflected ultrasonic energy pulses, each image frame corresponding to a predefined energy pulse characteristic, the imaging engine being further configured to identify prominent features of each separate image frame, the imaging engine being configured to provide display signals for simultaneously displaying the separate image frames as a composite image, the imaging engine is further configured to form the composite image by co-registering the separate image frames, such that features more prominent in a first image of the separate image frames are mapped to a second image of the separate image frames, and features more prominent in the second image are mapped to the first image, thereby including at least a portion of the prominent features of each of the separate image frames in the composite image.

2. The system of claim **1**, wherein the imaging engine is further configured to provide the imaging core with repeated sequence of energy pulses such that each sequence of energy pulses includes at least two pulses.

3. The system of claim **1**, wherein the imaging engine is further configured to provide the imaging core with repeated sequence of energy pulses, such that the energy pulses in each sequence having a different pulse energy.

4. The system of claim **1**, wherein the imaging engine is further configured to provide the imaging core with repeated sequence of energy pulses, such that the energy pulses in each sequence having a different frequency.

5. The system of claim **1**, wherein the imaging engine is further configured to provide the imaging core with repeated sequence of energy pulses, such that the energy pulses in each sequence having a different bandwidth.

6. The system of claim **1**, wherein the imaging engine is further configured to provide the imaging core with repeated sequence of energy pulses such that each sequence of energy pulses includes three pulses.

7. The system of claim **6**, wherein the imaging engine is further configured to provide the imaging core with repeated sequence of energy pulses such that

a first one of the three pulses has a first energy,

a second one of the three pulses has a second energy, a third one of the three pulses has a third energy, wherein,

the first energy is greater than the second energy, and the first energy is greater than the third energy.

8. The system of claim **1**, wherein the imaging engine includes a processor configured to process the reflected ultrasonic energy pulses in image frames and a detector that detects the varying characteristic in the reflected ultrasonic energy pulses, and wherein the imaging engine processes the frames according to the detected varying characteristic.

9. The system of claim **8**, wherein the imaging engine is further configured to process only reflected ultrasonic energy pulses having a common detected characteristic.

10. The system of claim **8**, wherein the imaging engine is further configured to provide a composite image based upon the varying characteristics of the sequences of reflected ultrasonic energy pulses.

11. A method comprising:

providing a catheter having an elongated body having a distal end and an imaging core configured to be inserted into the elongated body, the imaging core being configured to transmit ultrasonic energy pulses and to receive reflected ultrasonic energy pulses, an imaging engine coupled to the imaging core; and

providing the imaging core with energy pulses from an imaging engine coupled to the imaging core, the energy pulses being ultrasonic, to cause the imaging core to transmit the ultrasonic energy pulses, each energy pulse having a predefined energy pulse characteristic within a plurality of predefined energy pulse characteristics, the energy pulses being transmitted such that the associated predefined energy pulse characteristics are arranged in a repeating sequence, wherein

the imaging engine processes the reflected ultrasonic energy pulses in separate image frames, the separate image frames being acquired concurrently from the reflected ultrasonic energy pulses, each image frame corresponding to a predefined energy pulse characteristic, and wherein the imaging engine provides display signals for simultaneously displaying the separate image frames as a composite image, the imaging engine identifies prominent features of each separate image frame and forms the composite image by co-registering the separate image frames, such that features more prominent in a first image of the separate image frames are mapped to a second image of the separate image frames, and features more prominent in the second image are mapped to the first image, thereby including at least a portion of the prominent features of each of the separate image frames in the composite image.

* * * * *

专利名称(译)	用于共同配准成像的血管内超声系统		
公开(公告)号	US9808222	公开(公告)日	2017-11-07
申请号	US12/902460	申请日	2010-10-12
[标]申请(专利权)人(译)	SILICON VALLEY MEDICAL INSTR		
申请(专利权)人(译)	硅谷医疗器械，INC.		
当前申请(专利权)人(译)	ACIST医疗系统，INC.		
[标]发明人	MOORE THOMAS C WATERS KENDALL R REYNOLDS J STEVE LAM DUC H MASTERS DONALD		
发明人	MOORE, THOMAS C. WATERS, KENDALL R. REYNOLDS, J. STEVE LAM, DUC H. MASTERS, DONALD		
IPC分类号	A61B8/00 A61B8/12 G01S7/52 G01S15/10 A61B8/08 G01S15/89 A61B5/06		
CPC分类号	A61B8/4461 A61B8/0891 A61B8/12 A61B8/445 A61B8/463 G01S7/52074 G01S7/52071 G01S15/8952 A61B5/06 A61B8/0833 G01S15/102 G06T7/0012 G06T7/30		
优先权	61/250781 2009-10-12 US 61/256543 2009-10-30 US		
其他公开文献	US20110087104A1		
外部链接	Espacenet USPTO		

摘要(译)

一种具有导管的血管内超声成像系统，所述导管具有细长主体，所述细长主体具有远端和成像芯，所述成像芯设置成插入所述细长主体中成像核心布置成发射超声能量脉冲并接收反射的超声能量脉冲。该系统还包括成像引擎，该成像引擎耦合到成像核心并且被布置成向成像核心提供能量脉冲以使成像核心发射超声能量脉冲。能量脉冲按重复顺序排列，每个序列的能量脉冲具有不同的特性。可以处理反射的脉冲以提供由每个不同特征产生的图像的合成图像。